8-2024

An XRF Elemental Analysis of Prosser Molded Beads From Southwest Oregon

Michele Hoferitza
Utah State University

AN XRF ELEMENTAL ANALYSIS OF PROSSER MOLDED BEADS FROM SOUTHWEST OREGON

by

Michele Hoferitza

A thesis submitted in partial fulfillment
of the requirements for the degree

of

MASTER OF SCIENCE

in

Anthropology

Approved:

Judson Finley, Ph.D. Major Professor	Anna Cohen, Ph.D. Committee Member
Jacob Freeman, Ph.D. Committee Member	D. Richard Cutler, Ph.D. Vice Provost of Graduate Studies

UTAH STATE UNIVERSITY
Logan, Utah

2024

ABSTRACT

An XRF Elemental Analysis of Prosser Molded Beads

From Southwest Oregon

by

Michele Hoferitza, Master of Science

Utah State University, 2024

Major Professor: Dr. Judson Finley
Department: Anthropology

Prosser beads were made in France and Bohemia from the 1860's to the 1970's for trade in Africa and North America. Extensive sales and distribution networks were created by the Bapterosses (France) and Redlhammer (Bohemia) companies to both continents. Innovative manufacture techniques make Prosser beads visually and chemically distinct.

In this study, 175 Prosser Molded beads found in an archaeological context in southwest Oregon were examined with XRF. The purpose of the study is to determine if it is feasible to use elemental analysis as a tool to determine where and when Prosser beads were manufactured. Three groups of elements that are chemically related either naturally or by deliberate addition were examined to determine whether any of them showed statistically significant variation in the composition.

Prosser beads were made using powdered feldspar, quartz sand, and coloring agents. Major elements that occur naturally in feldspar are Si, Al, Ca, and K. Analysis of these four elements reveals a strong correlation of variance between Al and K.

Trace elements of Rb, Sr, Y, and Zr, associated with volcanic activity and with alkali replacement in feldspar were also analyzed to identify patterns of relationships between them. It was found that Rb was positively correlated with the other elements, and Sr had no relationship.

Coloring elements are added to the Prosser recipe to obtain various colors and shades. In examining these elements, Co content was found to vary widely in the blue beads. When compared to combinations of major elements, two clusters of beads appeared in the graphs.

Principal component analysis of Rb, Sr, Ca, and K showed that variations in Rb and K were correlated. Variation in Co content served as a control variable to reveal that these elemental combinations were not random, but the result of distinct manufacturing differences.

(65 pages)

PUBLIC ABSTRACT

An XRF Elemental Analysis of Prosser Molded Beads
From Southwest Oregon
Michele Hoferitza

Glass beads were brought to the North American continent by European explorers and traders beginning in the 17th century. Native Americans quickly adopted beads as trade commodities and personal ornaments. Prosser beads were made predominately in France and Bohemia from the 1860's to the 1970's and can be found in archaeological contexts from coast to coast. In this study, elemental analysis using X-Ray fluorescence (XRF) technology is used to determine if there is a way to chemically discern where and when the beads were made.

Statistical analysis of three categories of elements was done to determine whether the creation of a model of glass recipes for Prosser beads might be possible using XRF. Four major elements of feldspar, Si, Al, Ca, and K were analyzed, revealing a strong correlation between Al and K. Trace elements, Rb, Sr, Y, and Zr, which are associated with volcanic activity and alkali replacement in feldspar were examined, revealing that variation in Rb was strongly associated with Al. Finally, as a control, coloring elements that were intentionally added were examined, revealing that Co amounts had high variation, and were associated with statistical clusters of bead composition.

The study revealed that in the case of these beads, Al, K, Rb, and Co all varied together, and patterns of variation created clusters of beads in the analysis. This finding suggests the possibility that an elemental model is feasible. Ultimately, it may be possible to use a handheld XRF device in the field to determine quickly where and when, within a few decades, it was made.

The ability to distinguish this information about beads provides archaeologists with a powerful tool to trace patterns of trade and use of one of the most important commodities in Native American cultural adornment.

ACKNOWLEDGMENTS

I would like to thank my committee members, Dr. Anna Cohen and Dr. Jacob Freeman, for their support and for everything they taught me. Dr. Molly Cannon and Dr. David Byers contributed significantly to my education as well, and I appreciate everything they taught me about archaeology. I consider all of them to be my friends.

I thank Dr. Bruce Kaiser for his help, training, and support and for allowing me to use his Bruker Handheld XRF instrument under his supervision. I also thank Dr. Richard Shipley for making his bead collection available for study. Additionally, Dr. Elliot Blair from the University of Alabama provided support and insight in the use of the XRF including access to standards and suggestions for research which were greatly appreciated.

I especially want to thank Dr. Judson Finley for his contributions as my Committee Chair. He believed in me when others were skeptical, and provided uplifting advice when I was skeptical of myself. He connected me with all the right people and convinced me that I could be an archaeologist. I would not have come this far on my educational journey without his support.

Most importantly, nothing in my life would have been possible without my family. My parents have always supported every choice I've made. My children have been the center of my world. My husband Mark has been loyal, kind, and unwavering in his love and support for me as I have pursued higher education. I could not have finished this without him.

I would like to dedicate this manuscript to the generations of women in my family before and after me whose legacy of commitment to education will never be subdued.

Michele Hoferitza

CONTENTS

Page

LIST OF TABLES

Page

LIST OF FIGURES

Page

Introduction

Made in Europe for centuries, glass beads were produced in mass quantities for use as trade currency around the world as Europeans explored outside their continent in search of commodities and raw materials. Before Europeans arrived in North America, Indigenous people made beads from shell, bone, and stone, but glass beads quickly replaced traditional forms (Panich 2014). From the 15th to 20th centuries, European glass manufacturers in Italy, France, Bohemia, Germany, and the Netherlands increased supply to meet the growing demands of worldwide trade. In historical archaeology, the study of glass beads provides insight into the organization of trade networks between vendors, countries, and continents, as well as the economic development of consumer markets (Panich 2014). Beads also reflect cultural values and practices through their use in personal adornment and prestige signaling (Opper and Opper 1993). In the mid to late 19th century, high global market demand for glass beads was filled in part with mass-produced porcelain beads from France and Bohemia (Neuwirth 2011; Nourison 2001). These beads, called Prosser Molded beads, have been understudied in archaeological contexts (Kirkish 2014). This research is important because it lays the foundation for the study of anthropological questions about globalization of economy and culture, international trade, manufacturing communities of practice, and indigenous commoditization and use of trade beads on two continents. Because they were manufactured by the millions and are abundantly found in archaeological contexts in

North America and Africa, they provide a unique index to post-industrial international manufacturing and trade practices.

While glass beads are commonly found in the North American archaeological record (Hancock et al. 1994), Prosser beads were late arrivals. Consequently, when found, Prosser beads are often dismissed as chronological intruders in sites considered to be much older. Some researchers speculate that Prosser beads were sold by the Hudson's Bay Company (Kirkush 2014), but others point out the late manufacturing date may put them in the post-HBC era (Ross 1990). At least five different companies produced porcelain beads in Europe, but the industry was led by the Bapterosses Company in Briare, France, which was not only the first to produce them in 1864 but made them with high quality standards (Nourisson 2001). The Redlhammer Company in Gablonz, Bohemia entered the market in 1890 with more haphazard recipes, but with a wider variety of shapes and a marketing gusto that made it the prime competitor to the French producers (Neuwirth 2011). By the 1930's, global economic depression forced the competitors to become collaborators, forming a syndicate of porcelain bead producers, each providing product to common distribution companies (Nourisson 2001).

This thesis presents the results of an X-Ray fluorescence (XRF) analysis of 175 Prosser Molded beads from an archaeological context in southwest Oregon. The beads are from the private collection of Dr. Richard Shipley, and little is known about them beyond their approximate provenience near the confluence of the North and South Umpqua Rivers. This study presents the opportunity to examine the question of whether the factory of origin of Prosser beads can be determined through elemental analysis. Differences in geochemistry of raw material sources used in the factories in Briare and

Gablonz are expected to be indicated in the chemical composition of the beads. If such differentiation cannot be confirmed, it would suggest that in this case either a single company made the beads found in the collection or that chemical variability between the two manufacturers' recipes or raw material sources cannot be detected.

In this thesis, I first present an overview of the physical description of beads used by archaeologists in North America. Second, I outline the history of the development of Prosser beads and the companies and personalities that produced them. Third, I discuss the ways researchers categorize glass beads by physical and chemical attributes. Finally, I present a background on geochemical analytical methods in glass bead research, focusing on recent developments in XRF technology that enable rapid, inexpensive, and high-precision results, and note limitations that present challenges to this methodology.

Relationships of elements in the Prosser beads for this study are analyzed in three contexts. First, the elemental composition of feldspar, a main ingredient in Prosser beads, is considered in terms of the relative weights of the elements Al, Si, Ca, and K. For the purposes of this study, these four elements will be referred to as major elements as they are among the most common elements and form the primary ingredients in the Prosser recipe. Second, four trace elements (Zr, Y, Sr, Rb) associated with feldspars and with volcanic material are considered, as these can be geographically distinct and may act as markers for raw material sources (Heier 1962; Shackley 2011). Finally, chemicals used to create colors in the beads (Fe, Co, Cu, Zn, and Ti) are examined for variance. I suggest that variations of these three primary elemental components when considered together will provide the basis for differentiating Prosser Molded beads produced in the French and Bohemian factories. Information about the elemental composition of Prosser

beads from different locations is the first step in generating a model for identifying precise manufacturing locations of Prosser beads, millions of which were produced and distributed to worldwide markets. Multiple questions about technology, chronology, and trade are addressed by the study of beads (Dussubieux and Walder 2022). The process of creating beads, however, tells stories of invention, innovation, economic relationships, industrial production, and international commerce.

History, Chemistry, and Analysis of Prosser Molded Beads

Glass beads exist in archaeological context throughout the world, and date back as far as Roman times. The first formal classification system was published by Horace Beck (1926) after finding that archaeologists could not agree on simple bead descriptions, even making such imprecise reference in the literature to a "coloured Anglo-Saxon bead of the usual type" (Beck 1926:1). Beck's cumbersome system, however, stipulated descriptions about form, perforation, color, material, and decoration, and never caught on with North American researchers (Karklins 2012).

In the 1950's Canadian researchers Kidd and Kidd (1970) devised a hierarchal classification system that was based primarily on manufacturing technique, then physical characteristics of shape, size, and diaphaneity. Kidd and Kidd (1970) acknowledge that the sheer variety of extant beads exceeds individual descriptions. Their system, which is based on the examination of 500 bead types, was intentionally designed to be expandable

(Karklins 2012). The Kidd and Kidd system distinguishes between drawn and wound beads, depending on the manufacturing technique used. In drawn beads, a tube or cane of hot glass is pulled between two people and stretched to a desired length or diameter, then left to cool. Once cooled, the tubes are cut into segments of desired length, and sharp edges are often heat rounded by various methods. Wound beads, on the other hand, are made by winding hot glass around a wire or mandrel. Such beads can be decorated before cooling and are often referred to as lampwork (Kidd and Kidd 1970; Karklins 2012).

Karklins (1985) provided extensions to the Kidd and Kidd classification system to include wound-on-drawn, mold-pressed, blown, and Prosser Molded beads (Karklins 2012). Mold-pressed beads were manufactured primarily in Bohemia beginning in the 19th century and are often referred to as Czech beads (Neuwirth 2011). Blown beads were made by blowing air into a heated glass tube to create free shapes or blown into a mold. Because of their delicate nature, blown beads are rarely found intact in archaeological contexts (Karklins 2012).

Prosser Molded beads are not made from molten glass but are instead created by compressing powdered ingredients into a mold, then firing them in a kiln. Though Karklins (2012:74) refers to Prosser Molded beads as "technically ceramic," they are included as a separate bead classification because of their glassy appearance due to high Si content. Though other classification systems have been suggested that depend on physical attributes including relative size and function of beads, the Kidd and Kidd system as updated by Karklins has remained the most definitive classification tool for North American bead research (Hancock 2005; Sempowski 2000).

A Manufacturing History of Prosser Beads

In 1840, Richard and Thomas Prosser obtained patents in England and the US, where each lived respectively, for an automated process of making porcelain buttons (Sprague 2002). The original patent described the use of clay or "clayey earths", flint, and feldspar as base materials. In the original processes, the dry powdered ingredients were compressed in a mold without added liquid. With enough pressure, the clay material holds the shape of the mold, and the button can be turned out onto a tray for firing. The American Prosser button industry was very successful, but dwindled in England when the European market was taken over by a French manufacturer, Jean-Felix Bapterosses (Sprague 2002).

After working for a short time for the Minton Company in England, which produced Prosser buttons, Bapterosses obtained a European patent in 1844 for a revised process of making buttons, tiles, and beads that represented several improvements to the original Prosser system (Sprague 2002). The evolved process used powdered feldspar, calcium fluoride, silica sand, and various ingredients as needed to provide color (Karklins 2012; Opper and Opper 1991). The powder mixture was combined with a liquid to make a paste that was then pressed into a two-part gang mold to create as many as 500 beads at one time (Kirkish 2014). Bapterosses was the first to use milk as a liquid binding agent, which improved the plasticity of the material (Sprague 2002). The molded mixture was then released onto a tray which was fired in a kiln. The resulting beads have a raised equatorial band where the two mold pieces meet, and a glassy, opaque appearance. They

are smooth on the top side but have a characteristic “orange peel” texture on the bottom where the bead sat on the tray in the kiln (Kirkush 2014; Kaspers 2011).

Bapterosses was an aggressive entrepreneur, and by 1851 he had purchased and renovated a failing ceramics factory in Briare, France, south of Paris along the River Loire about 40 miles east of Orléans. The more efficient production and cheaper labor in France allowed Bapterosses to undercut the English market, which stopped production of buttons by 1848. Prosser bead production in Briare began in 1864 and beads were widely distributed to American and African markets under the Bapterosses brand labeled “oriental” beads. With this success, the factory at Briare grew to include a dairy farm that produced milk for manufacturing operations, coal-fired kilns, a carpentry shop, a woodlot to make containers, its own printing press to produce marketing materials, and, ultimately, even an electricity generator (Nourisson 2001). Bapterosses was also a respected philanthropist, helping to build a school, hospital, church, and housing for workers, and supporting the arts and athletic recreation activities for the entire community (Nourisson 2001; Opper and Opper 1991).

The nearby Loire River and local canals provided efficient shipping pathways for raw materials. In 1879, Paul Yver, Bapterosses’ son-in-law, traveled to Norway in search of feldspar sources. After rejecting an alternative in England, Yver purchased a Norwegian mine which supplied minerals to Briare until after World War II (Nourisson 2001). In addition to feldspar, quartz sand was a necessary ingredient. An excellent and local source for sand was the Fontainbleau Sand Formation in the Paris Basin, well known for high quality white silica sand with few impurities (Thiry and Marechal 2001).

While the Prosser bead production in Briare was developed by Bapterosses' effective entrepreneurship, the industrial process in Bohemia had more complex roots. The glass-making industry in the area dates to 1550 when new Venetian red glass production began competing with local stone cutters' garnet production (Kaspers 2014, Neuwirth 2011). By the 18th century, German glassmakers in the city of Gablonz (now Jablonec nad Nisou, Czechia) were making composition glass with various amounts of lead, resulting in sparkling colors and clear crystal, rivaling even the Venetian glass industry. Novel manufacturing techniques developed for pressing glass into molded shapes and for facet grinding helped make beads and other small glassware a popular and profitable regional industry (Neuwirth 2011).

Eduard Moritz Redlhammer, a Bohemian businessman, established a glass export company in Gablonz in 1882. His two sons, Eduard and Albert, however, lost a great deal of money in their father's export business. The senior Redlhammer, who was quite wealthy, offered his sons a final opportunity and financed a venture in bead manufacturing (Nourisson 2001). The success of the Bapterosses Company caught their attention, and the Redlhammer brothers began experimenting with porcelain beads, beginning production in 1890. The buttons and beads they produced were lower quality than those made in Briare, but their trade connections provided good marketing opportunities in India and Africa. Gablonz became known for porcelain beads, and the Redlhammer Brothers Company became the primary competition for the Bapterosses. Continuous improvements to the process of mass production machinery supported the expansion of the industry, and a new factory built in 1905 was expanded in 1908 (Neuwirth 2011). The market for Prosser beads and buttons expanded rapidly, largely due

to the astute business sense of Bapterosses and the Redlhammer brothers. Other factories making similar porcelain products existed, most notably the Risler Company in Freiburg, Germany, but none matched the volume and success of these two (Sprague 2002).

The first half of the twentieth century was a series of booms and busts for the Prosser bead industry. European colonialism in Africa provided access to an eager market for the colorful, opaque beads, called "ushanga maka" in Swahili (Karklins 1992). Special shapes were made for the African market including triangle-shaped talhakimts worn as pendants or hair ornaments by Touareg tribes (Kaspers 2014). In the United States, Native Americans regularly incorporated beads into cultural dress and accessories by the 19th century (Orchard 1975), and Prosser beads were inexpensive and readily available. For Middle East customers, Islamic prayer beads were pressed with Quaran verses for Mecca pilgrimages (Kaspers 2014). For Asian markets, imitation coral molded to look like branches were produced along with beads in a variety of oriental and Hindu motifs (Kaspers 2011). Scarab beetles, sarcophagi, and other Egyptian Revival themed beads were popular in Europe and America in the 1920's after the discovery of the tomb of King Tutankhamun (Kaspers 2014).

Some cooperation developed in the industry as distributor networks were formed and included products from multiple manufacturers (Kaspers 2011). Trade relationships fractured with World War I, however, and bead production began to decline as raw materials were diverted to war efforts. A short decade of economic recovery after the war was undercut by the Great Depression in the 1930's, and World War II further decimated both access to raw materials and accessible markets. Decolonization in Africa and Asia in the 1960's and 1970's pushed the bead industry into further decline.

After World War II, people of German descent living in Gablonz were exiled and the communist government in the newly created Czechoslovakia took over industrial manufacturing. The Redlhammer Brothers Company was absorbed by Jablonex, the state-run bead company, which was later sold to the Preciosa company after the Velvet Revolution of 1989. Preciosa stopped making Prosser beads in 1993 but continues to sell traditional Czech glass beads worldwide. The post-war decline in bead trade forced the factory in Briare to access less expensive mineral materials from the Massif Central and Pyrénées mountains in the south of France (Nourrisson 2001). The Bapterosses Company stopped production of beads in 1962 but continued to make "emaux de Briare" mosaic tiles for another twelve years. Production operations ceased in 1974 when the Briare factory equipment was sold and moved to Morocco.

Geochemical Approaches to the Analysis of Glass Beads

Advances in geochemical analytical methods over the last 25 years have enabled researchers to move beyond descriptive classifications and consider the spatial and temporal variability in bead production and exchange based on their geochemical composition (Hancock 2005). The primary elements in glass are ubiquitous, but the combination of elements into glass recipes is almost limitless (Blair 2022). Glass is composed of what is referred to as a "network former," typically Si or Pb, a "network modifier" or flux, usually an alkali such as Na or K, and a stabilizer, usually Ca (Blair 2022; Kidd and Kidd 1970). Additional elements may be added acting as opacifiers, de-opacifiers, and coloring agents. Glass bead recipes can be quantified based on the major

and minor elemental composition of network formers and network modifiers, as well as the trace elemental composition of opacifiers and coloring agents (Blair 2022).

Chemical analysis of ancient glasses has been a subject of ongoing scientific study since the 1960's (Brill 1999). The Corning Archaeological Reference Glasses, produced by the Corning Museum of Glass, are widely used to categorize antique glasses by chemical composition and provenance (Brill 1999). These standards were created to replicate elements in glass at the major, minor, and trace concentrations. Corning A and B glasses are sodium-rich lime silicate glasses that resemble Egyptian, Mesopotamian, Roman, Byzantine, and Islamic glass. Corning C is high in lead and barium and reflects glasses from East Asia. Corning D is a potash-lime silicate glass that is like medieval glasses produced in Europe (Adlington 2017; Brill 1999; Vicenzi et al. 2002).

Glass made in the historical era, however, contains more complex elemental combinations representing recipes that varied over time and space, as chemical science was not exact (Kidd and Kidd 1970). Analyzing post-Medieval heritage glasses through elemental composition techniques has become increasingly more accessible to archaeologists via inexpensive, portable XRF equipment. Referring to the combination of formers and modifiers, Blair (2022) categorizes heritage glasses into four categories: soda glasses, potash glasses, lead crystal glass, and lead-barium glass. Prosser beads, however, do not fall neatly into any of these categories.

Prosser beads have been called "agate" or "stone" beads, porcelain beads, or tile beads (Karklins 2012, Kirkish 2014). The use of stone and porcelain as descriptors is likely in reference to the use of clay, feldspar, and quartz as main ingredients in bead recipes. The original Bapterosses patent listed the raw materials used as 70% kaolin clay,

15% feldspar, 9% calcined gypsum, and 6% calcium carbonate (Nourisson 2001). Later recipes do not mention clay but include Fontainbleau Sand (Opper and Opper 1991). Using energy dispersive XRF in a laboratory analysis, Sprague (1983) concluded that Prosser buttons and beads are chemically identical to glass but maintain a crystalline structure absent in glass. As a result, archaeologists refer to them as ceramic (Karklins 2012; Sprague 2015). Nevertheless, with a high content of Si, often the primary foundational ingredient in glass, Prosser beads are included in the study of glass beads (Karklins 2012; Sprague 1983). Feldspar, quartz sand (Si) and sometimes kaolin clay (Al and Si) were used as basic ingredients for Prosser beads, which should be accounted for in the elemental analysis. The purpose of this study is not to identify specific locations of sources for quartz, clay, or feldspar used to make the beads, but rather to determine whether elemental analysis will indicate that distinction can be made between two or more manufacturing origins.

Historical archaeology has the advantage of combining known information from written records with material items informing and expanding understanding of the documentary record (Andrén 1998). One disadvantage is that objects may be collected and associated with incorrect or incomplete documentation. For example, museums in both Briare and Jablonec are dedicated to the bead, button, and tile industry that built wealth and prosperity in each city. Nevertheless, each museum includes bead sample cards from multiple manufacturers and distributors, or that are unmarked, making research difficult and confusing (Kaspers 2011). Documentation regarding raw material sources exists in Briare, but such information is not available for other Prosser factories.

"Company history" documents are written by descendants of the founders or by employees and are often more marketing materials than objective observations.

This tension between what is known through documentation or texts and what is observed in the material record is referred to by Andrén (1998) as the paradox of historical archaeology. Archaeologists have increasingly turned to elemental composition to supplant gaps in written information (Burgess and Dussubieux 2007; Dadiego 2021; Hancock 1994). Recent studies have shown that chemical analysis can provide information about chronology, manufacturing technology, and provenance of glass (Adlington et al. 2019; Blair 2017; Hancock 1997). Specific glass manufacturers usually cannot be easily identified by chemistry in part because of the traditional secrecy surrounding recipes (Blair 2017). Nevertheless, in a review of neutron activation analysis (NAA) studies, Hancock (2005:55) surmised that elemental analysis may lead to identifying countries of origin, providing "fingerprints for tracking glass beads." A notable example showed that correlations between Co and As in beads from two different sites in Ontario indicate the coloring agent could be associated with the Hartz Mountains of Germany (Hancock et al. 2000).

Hancock et al. (1994) determined that 16th century beads found in the eastern Great Lakes area of North America contained lower amounts of calcium, chlorine, and sodium, and higher amounts of copper than later 17th century beads. While this result suggests that these four elements could be used to establish a chemical chronology for beads found in the area, the study could not conclude whether the variation was due to changes in recipes, changes in raw material sources, or the establishment of new factories or distribution networks. Nevertheless, Hancock et al. (1994) were optimistic to find that

chemical variations could reflect chronological distinctions in beads of visually similar colors or types.

Sempowski et al. (2000) studied white glass beads from 15 Seneca Iroquois sites in western New York spanning seven known time periods. They found a gradual transition from the use of tin to antimony as a glass opacifier during the early part of the 17th century. They conclude that the shift was in response to either cost or availability changes of raw materials to Dutch bead manufacturers. In a study of white glass beads from a Spanish-colonial site in Georgia, Blair (2017) demonstrated that the change in opacifier elements from tin to antimony, and later to arsenic and then fluorine was a reliable chronological marker.

Finally, the study of chemical compositions of archaeological materials requires a focused statistical analysis of the elements present in the material. Principal component analysis (PCA) is commonly used to seek patterns among large element groups. Michelaki and Hancock (2011), however, demonstrated that simple bivariate plots of geochemically related elements can suggest diagnostic elements that reveal patterns in the data that are obscured by multivariate methods.

X-Ray Fluorescence Analysis

Elemental analysis of objects can be done by a variety of methods, but historically, available technology was expensive and had limited accessibility (Glascock 2011; Walder 2018). Advances in XRF technology have provided archaeologists with a low-cost, portable method of chemical analysis. Elemental studies of glass beads have

been done using Instrumental Neutron Activation Analysis (INAA) (Hancock et al. 1994; Kenyon et al. 1995), Laser Ablation Inductively Coupled Mass Spectrometry (LA-ICP-MS) (Dadiego et al. 2021; Walder 2018), and XRF (Blair 2017; Sprague 1983). XRF can provide reproducible results that are comparable to NAA and LA-ICP-MS (Glascock 2011; Walder et al. 2021).

Energy-dispersive XRF (ED-XRF) provides information about the elements present in an object through the introduction of an X-Ray beam, and the analysis of the released energy called fluorescence. An X-Ray is high-energy, high-frequency photon radiation (Shackley 2011). The radiation excites the electrons of the atoms of the target material, causing some of them to escape the orbit of the atom. When an electron escapes a lower orbital shell closer to the nucleus, an electron from a higher shell replaces it, radiating energy in the form of photons that leave the material. The energy is detected and analyzed by the XRF device and translated by software into spectra that represent the number of photons (y-axis) for each energy level measured in kilovolts (keV) (x-axis) (Drake and MacDonald 2022; Shackley 2011). Individual elements reflect photons at specific energies and their relative presence is indicated by photons under the curve on the spectra.

The low cost and portability of XRF devices make the technology a good choice for archaeologists in some contexts, but several limitations should be noted. XRF measures only the surface of the artifact, depending on the density of the material and the elements being examined. Homogeneity of the material is important, as clusters of elements in the material could bias results. Lighter elements including sodium and magnesium cannot be detected unless the sample is evaluated in a helium environment

(Blair 2022). Prosser beads typically do not have a surface coating and like glass are sufficiently homogenous. However, the deficiency of sodium and magnesium in this analysis is noted as a liability.

Increased access to XRF technology has given researchers a new way to analyze and categorize bead assemblages through the identification of elements that make up the bead either as naturally occurring components of raw materials, or as something deliberately added for color or opacity. The limited nature of the recipe for Prosser beads increases the likelihood of distinguishing between natural and intentional components.

Methods

The beads used in this study are from the private collection of Dr. Richard Shipley of Centerville, Utah. Dr. Shipley's collection, purchased from estates of collectors, includes stone points and arrowheads from around the Great Basin as well as glass trade beads and various other artifacts from the region. The beads chosen to study were two strands from a display case labeled Frame 131 (Figure 1), identified by Dr. Shipley as coming from Ron Rathbone, a collector in Twin Rivers, Oregon. The beads are identified as Prosser beads by the presence of a wide equatorial raised band left by the mold that is the primary diagnostic element for this type (Karklins 2012). Figure 2 shows the band in detailed pictures of some of the Shipley collection beads. The beads were removed from the

Figure 1. Frame 131 from Richard Shipley Collection. The frame includes African trade beads, shell beads, padre beads, Prosser beads, mother-of-pearl beads, and arrow points.

Figure 2. Detail picture of Prosser beads. Equatorial band is visible which is diagnostic of Prosser Molded bead types. The beads are round to slightly oblate in shape.

nylon lines and each bead was numbered, weighed in grams, and measured with a caliper in millimeters for height, measuring along the axis of the hole, and for width, measuring the equatorial axis.

X-Ray fluorescence analysis was conducted using a Bruker Handheld energy dispersive XRF Spectrometer Tracer 5i model, serial number 900F4939. While this instrument is "handheld," it contains the same technology and instrumentation as a bench-top ED-XRF instrument, unlike earlier versions of handheld equipment that is called portable or "pXRF." As a result, there is sometimes confusion over terminology as older pXRF technology often did not match the capabilities of the ED-XRF, especially in the measurement of lighter elements. Newer technology has improved the instruments in the last two decades, however, and portable systems have the same operational physics and analytical capabilities as traditional non-portable systems (Johnson et al. 2021). The instrument used in this study is considered laboratory-grade and is capable of measurement voltages up to 50kV. It was used in a laboratory setting and is referred to hereafter simply as the XRF or the XRF instrument.

The reliability of the XRF, or the ability to reproduce results, is specific to each instrument, within a small margin of error (Blair 2022; Yatsuk et al. 2022). That error is mitigated in the data through the calibration of results by using the same instrument to scan standards that have known element weights that were verified by more sophisticated technology. In the case of glass, 300 Heritage Glass standards are available that were analyzed by LA-ICP-MS (Blair 2022). The calibration of data uses the known element weights to adjust the measured unknown weights of elements and convert the photon

count to parts-per-million (PPM) values, which allows comparison of elements in standardized units.

To maximize accuracy, each bead in this study was scanned twice in the same position at different voltage settings. The low voltage scan was done in a plain air atmospheric path using an X-Ray tube setting of 15 kV (high voltage) and 10 μA (current) with no filter. The high voltage scan was done in a plain air atmospheric path using up to 50 kV (high voltage) and 35 μA (current) with a filter composed of 100 μm Cu, 25 μm Ti, and 300 μm Al. All assays were conducted using a 3-x-3 mm spot size for 30 seconds. The spectra generated by the scan were converted into values reflecting the photon count under the peak created for each element using the Bruker S1PXRF software, version 1.8.0.136.

Raw spectra data provide relative qualitative information about elements found in each bead but do not provide a standardized way to compare element weights among different beads. To compare elemental composition between beads, photon counts must be converted to PPM values. This conversion requires the XRF instrument be used to scan standards samples with known values to provide the relative baseline for results comparison (Blair 2022). For this study, twenty glass samples were scanned from the Heritage Glass standards collection of Dr. Elliot Blair, who also provided the known element weights generated through LA-ICP-MS. The spectra generated by the scan of the standards and the known values were combined into formulas in an Excel spreadsheet provided by Dr. Bruce Kaiser to calculate PPM values.

Results

The Prosser Molded beads selected for study are of various sizes and consist of eight colors (Table 1). Three clear glass beads and two cobalt drawn faceted glass beads were excluded from the study as they are not Prosser beads. The beads range in size with height from 3.75 to 6.15 mm, width from 4.21 to 6.62 mm, and weight from 1.0 to 5.2 grams. Measurements show that the beads are round to oblate, as the height of most beads measured from the top to bottom of the bead hole is slightly smaller than the width of the bead. The beads in this study therefore are categorized as PMIa (round)-PMIb (oblate) according to the Kidd Classification System (Karklins 2012).

Table 1. List of colors of beads included in Shipley Collection, Frame 131.

Color	Number of Beads
Black	8
Blue	102
Burgundy	7
Light Green	12
Turquoise	12
Olive Green	25
White	9

The spectra generated by the XRF assays are a qualitative representation of elements present in the beads. Each element corresponds to a voltage peak intensity that varies according to the percentage of that element in that specific bead. Although the ARTAX software restricts the display of spectra to 100, cluster patterns can be observed

in several elements (Figure 3). A closer view of the spectra for volcanic trace elements further reveals that group patterning exists most strongly in Rb (Figure 4).

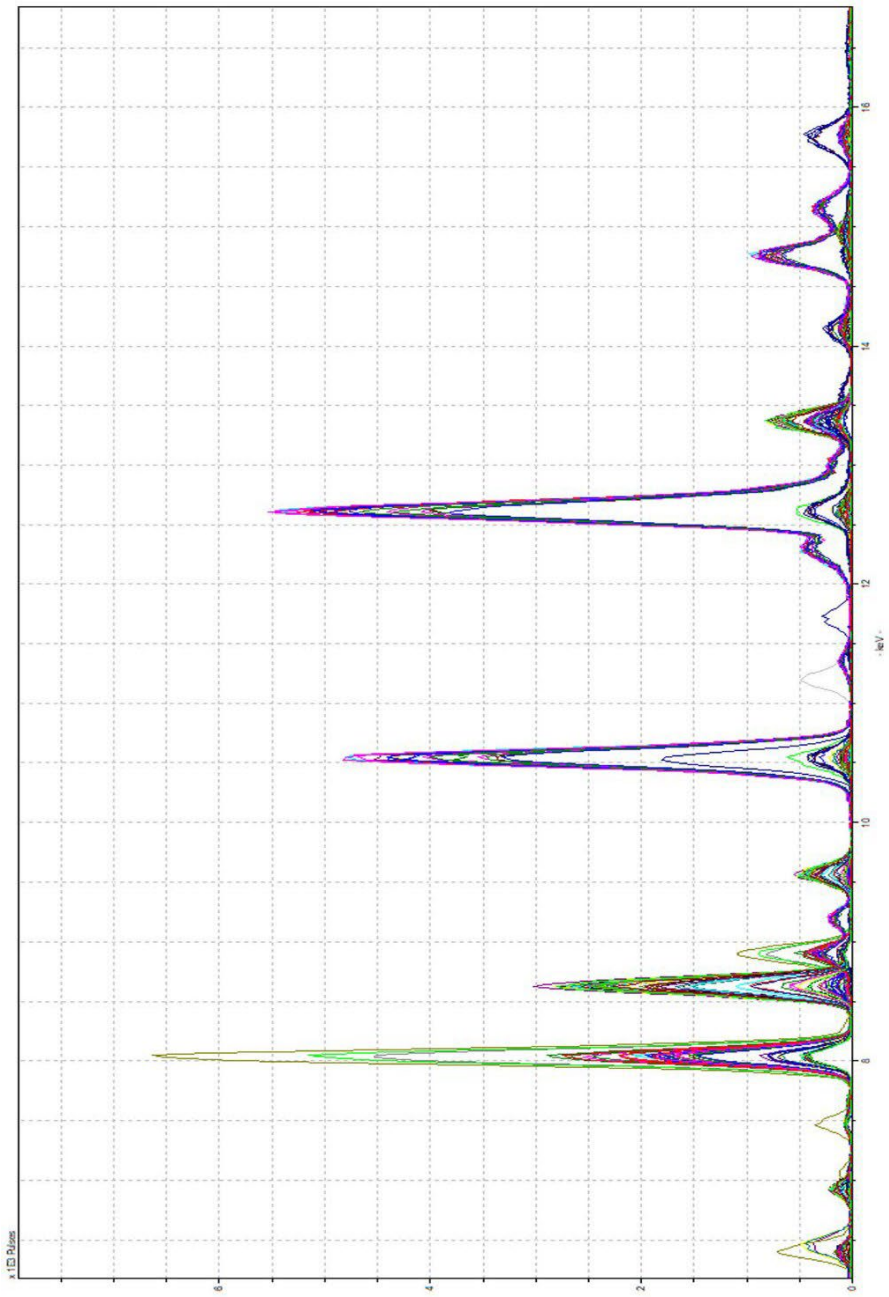

Figure 3. Display of spectra from high-voltage scans. ARTAX software can display up to 100 spectra on one screen. The colors are not associated with bead color, rather represent individual spectrum.

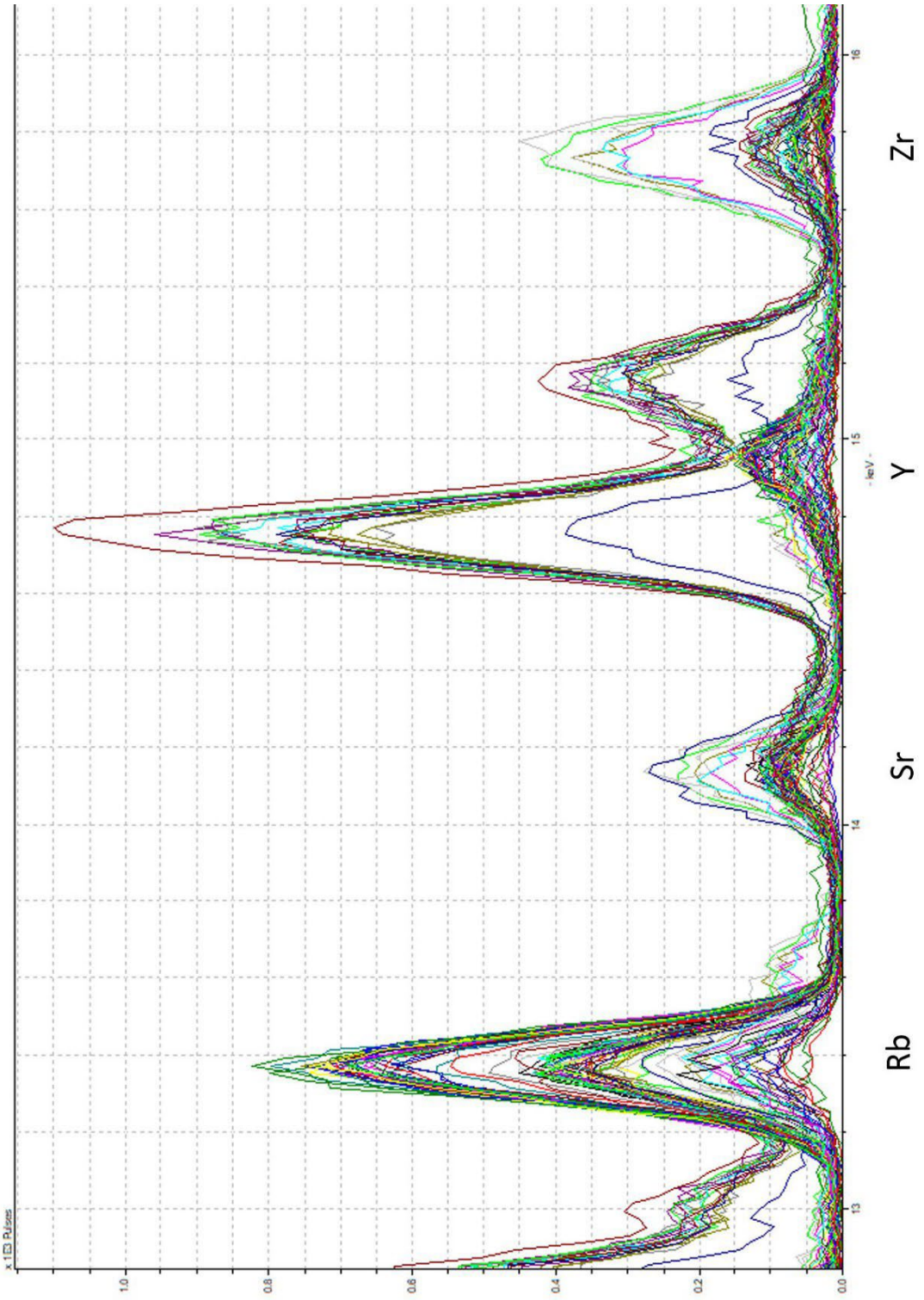

Figure 4. Detail of spectra portion showing trace elements of Rb, Sr, Y, and Zr. ARTAX software can display up to 100 spectra on one screen. The colors are not associated with bead color, rather represent individual spectrum.

The analysis successfully generated PPM values for the major elements of Si, Ca, K, and Al by bead color (Table 2). The analysis also produced PPM values for minor elements of Fe, Co, Ni, Cu, Zn, As, Pb, Mn, and Ti by bead color (Table 3). The elements Rb, Sr, Y, and Zr are also present in trace amounts (Table 4). The concentrations of the four major elements in each bead were analyzed by bead color (Figure 5). A one-way analysis of variance (ANOVA) for Si shows that black, burgundy, and turquoise beads have mean distribution of concentrations above the total mean of 360,481 PPM ($f=16.09$, $df=6$, $p<0.001$). For Ca, blue, olive, and white beads all have mean distributions above the total mean of 382 PPM ($f=9.28$, $df=6$, $p<0.001$). Blue beads are the only color with concentrations above the means for K (mean=40,635 PPM, $f=16.36$, $df=6$, $p<0.001$) and Al (mean=51,291 PPM, $f=16.23$, $df=6$, $p<0.001$). Blue beads also have the widest distribution of concentrations in all four elements.

One-way ANOVA analysis was also done for minor elements (Table 5), which reveals strong visual patterning by bead color in several elements (Figure 6a and 6b). Blue beads have the greatest variation of Co and olive beads have the greatest variation of As. Mn shows low concentrations in all except the black beads, and is absent in blue, light green, olive, and white beads. White beads show high concentrations of Ti, which is absent in black, burgundy, and turquoise beads. Concentrations of Fe are below the mean for blue and turquoise beads and above the mean in black, olive, and white beads, with burgundy and light green showing the element more evenly distributed. Zn and Cu have generally even distribution of concentrations, although turquoise beads are low in Zn, and burgundy, light green, and olive beads are all above the mean for Cu content. Concentrations of Pb are evenly distributed in black, blue, and burgundy beads, but light

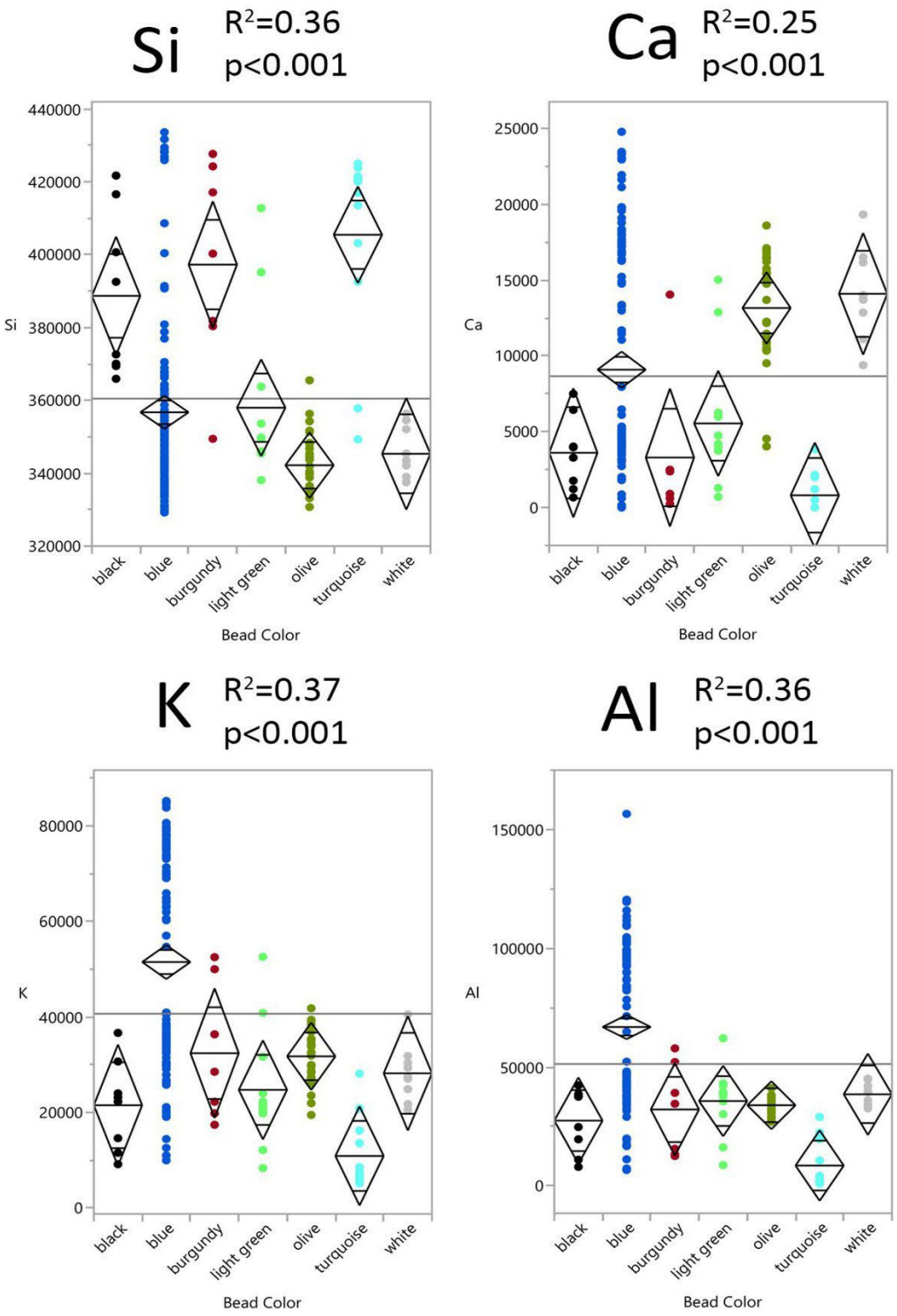

Figure 5. Box plots for major forming elements Si, Ca, K, and Al by bead color. Gray horizontal line is the mean for all beads. Each diamond shows the mean and standard deviations for each bead color.

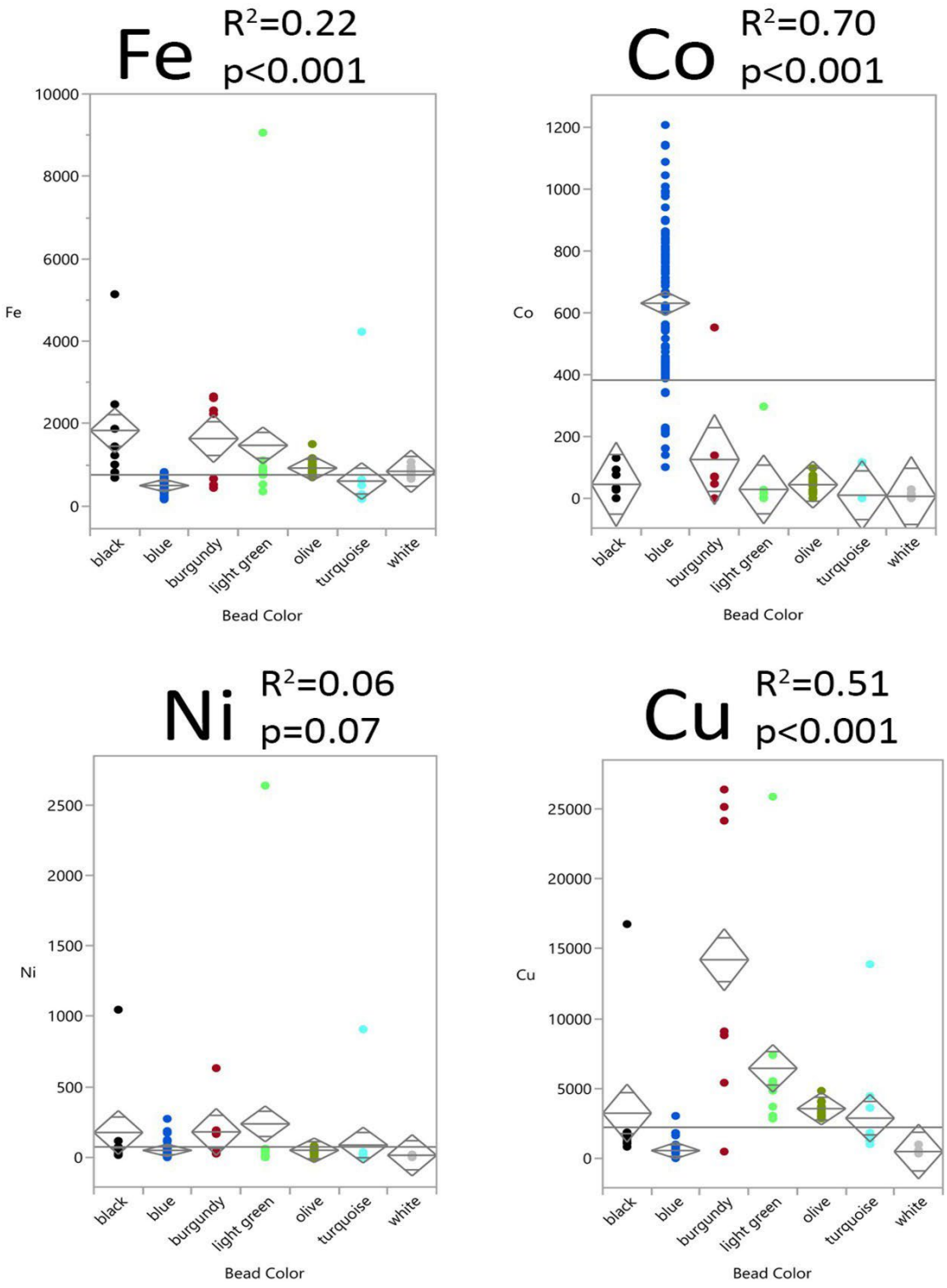

Figure 6a. Box plot charts for minor elements Fe, Co, Ni, and Cu by color. Gray horizontal line is the mean for all beads. Each diamond shows the mean and standard deviations for each bead color.

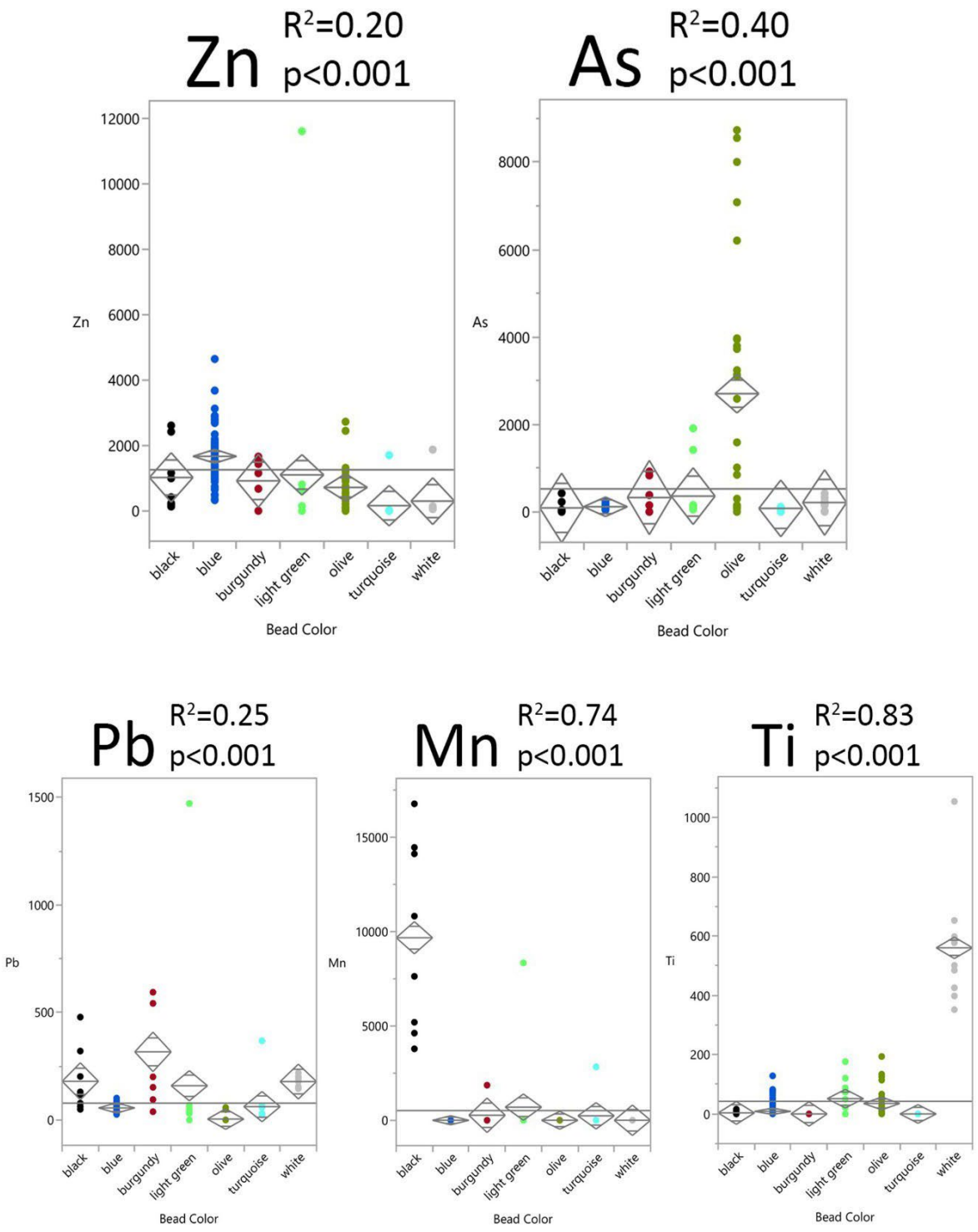

Figure 6b. Box plot charts for minor elements Zn, As, Pb, Mn, and Ti by color. Gray horizontal line is the mean for all beads. Each diamond shows the mean and standard deviations for each bead color.

Table 2. Summary of major element concentrations by bead color.

Element		Black	Blue	Burgundy	Light Green	Olive	Turquoise	White
Si	Min	365944.64	329234.64	349456.56	338116.27	330748.79	349291.87	337514.77
	Max	421721.33	433631.51	427669.29	412790.44	365509.94	425005.58	356348.04
	Median	382588.79	349838.69	400291.52	349793.46	340058.22	418541.74	343455.55
	Mean	388702.28	356738.64	397282.81	357993.67	342193.47	405472.88	345342.34
	Std Dev	22428.01	25912.12	28475.17	22867.72	8628.94	26043.08	7303.45
Ca	Min	665.20	0.00	237.79	705.24	4026.24	0.00	9386.52
	Max	7497.04	24767.78	14041.25	15011.02	18593.03	3852.24	19316.49
	Median	3628.37	4885.71	2379.73	4092.44	14217.61	0.00	13744.19
	Mean	3608.78	9088.82	3297.38	5544.96	13153.34	807.98	14088.18
	Std Dev	2427.89	7361.91	4830.83	4257.85	3703.53	1254.86	2964.83
K	Min	9129.51	9945.69	17388.18	8309.54	19440.00	5131.01	20526.73
	Max	36619.02	85230.21	52475.11	52539.00	41776.45	28090.16	40503.98
	Median	22673.67	40701.00	28488.52	21692.99	32207.79	7135.87	27394.06
	Mean	21474.21	51458.44	32374.45	24689.42	31709.99	10859.97	28161.28
	Std Dev	9423.88	22439.60	14321.09	12022.89	5758.35	7354.30	5962.22
Al	Min	7997.97	6692.66	12563.86	8745.87	27048.31	924.05	32657.90
	Max	42290.37	156589.21	57882.56	62111.81	41172.01	28994.73	45134.38
	Median	31148.40	58582.66	34564.30	38580.59	34368.10	3489.08	39560.66
	Mean	27475.28	66873.28	32163.63	35718.68	33956.36	8554.52	38560.54
	Std Dev	13489.54	32614.67	18841.35	13653.04	3667.28	9684.50	4879.52

Table 3. Summary of minor elements in PPM by bead color.

Element		Black	Blue	Burgundy	Light Green	Olive	Turquoise	White
Fe	Min	689.23	164.82	443.77	357.51	698.04	175.78	662.71
	Max	5141.29	827.18	2662.23	9060.42	1505.09	4231.28	1072.76
	Median	1340.32	524.18	2235.48	819.52	889.77	211.68	832.45
	Mean	1836.37	499.11	1638.52	1475.35	924.21	607.82	844.00
	Std Dev	1457.54	136.95	1038.45	2396.20	174.31	1150.43	122.12
Co	Min	0.00	100.74	0.00	0.00	0.00	0.00	0.00
	Max	130.37	1208.16	552.79	296.91	97.27	116.74	28.90
	Median	30.09	663.91	68.39	0.00	44.57	0.00	0.00
	Mean	44.89	631.28	125.28	28.45	43.86	9.73	6.15
	Std Dev	49.37	245.76	194.40	84.97	25.04	33.70	10.00
Ni	Min	16.36	0.00	25.83	0.00	0.00	0.00	0.00
	Max	1047.72	273.10	632.80	2638.30	81.28	908.92	22.62
	Median	51.48	48.53	165.56	9.91	51.89	10.70	16.16
	Mean	175.91	49.06	180.19	237.16	49.86	86.41	14.24
	Std Dev	353.77	39.53	212.28	756.44	18.25	259.28	7.74
Cu	Min	823.29	0.00	475.84	2831.97	2843.94	1003.03	333.68
	Max	16766.25	3032.82	26406.86	25892.93	4840.84	13890.37	989.34
	Median	1306.44	481.89	9084.61	5190.01	3432.75	1492.25	425.49
	Mean	3226.98	547.80	14215.89	6437.45	3551.36	2870.21	476.89
	Std Dev	5480.78	325.01	10720.35	6269.19	543.06	3626.23	204.98
Zn	Min	131.37	327.64	0.00	0.00	0.00	0.00	54.70
	Max	2608.03	4642.02	1657.17	11605.01	2723.81	1702.76	1870.24
	Median	704.87	1708.53	1151.75	0.00	545.97	18.93	111.29
	Mean	1018.56	1666.66	916.71	1099.23	715.63	157.83	296.96
	Std Dev	997.65	702.15	701.24	3320.07	690.22	486.62	590.67
As	Min	0.00	42.03	0.00	53.20	0.00	0.00	0.00
	Max	424.15	235.12	921.24	1910.41	8734.17	112.10	420.82
	Median	10.61	110.86	149.14	102.46	2087.57	79.98	178.78
	Mean	89.60	115.86	326.65	358.65	2703.53	78.07	211.54
	Std Dev	155.67	35.19	401.04	619.13	2918.68	26.94	154.32
Pb	Min	49.43	25.86	38.42	0.00	0.00	23.98	145.53
	Max	478.05	101.33	594.81	1471.38	57.75	367.82	218.44
	Median	123.88	62.36	200.17	46.17	0.00	28.87	180.76
	Mean	179.75	55.95	316.51	159.04	4.07	61.88	178.39
	Std Dev	149.59	17.67	249.15	413.84	14.46	97.25	23.75
Mn	Min	3782.19	0.00	0.00	0.00	0.00	0.00	0.00
	Max	16744.68	0.00	1858.01	8328.22	0.00	2826.57	0.00
	Median	9207.85	0.00	0.00	0.00	0.00	0.00	0.00
	Mean	9659.36	0.00	265.43	694.28	0.00	235.55	0.00
	Std Dev	5046.18	0.00	702.26	2404.07	0.00	815.96	0.00
Ti	Min	0.00	0.00	0.00	0.00	0.00	0.00	351.83
	Max	16.04	128.39	0.00	176.44	193.62	0.00	1053.86
	Median	0.00	0.00	0.00	35.52	11.46	0.00	501.04
	Mean	3.50	8.73	0.00	51.50	35.31	0.00	560.27
	Std Dev	6.05	23.39	0.00	58.56	51.80	0.00	209.49

Table 4. Summary of trace elements in PPM by bead color.

Element		Black	Blue	Burgundy	Light Green	Olive	Turquoise	White
Rb	Min	22.75	53.23	50.42	21.45	51.23	26.64	79.94
	Max	204.31	457.40	365.47	397.76	240.41	172.84	124.51
	Median	53.79	252.85	194.23	54.98	195.56	40.29	95.94
	Mean	76.53	241.21	206.36	101.75	186.51	64.25	98.33
	Std Dev	61.12	100.63	130.04	107.33	47.35	49.26	13.68
Sr	Min	0.00	0.00	0.00	0.00	0.00	18.15	0.00
	Max	87.13	76.25	76.55	84.04	75.53	78.73	41.85
	Median	71.58	0.00	0.00	73.18	0.00	77.84	12.50
	Mean	50.13	10.72	28.99	55.57	5.85	68.54	14.40
	Std Dev	41.96	20.44	36.60	34.01	20.31	18.70	16.14
Y	Min	3.36	4.40	5.16	3.23	4.79	3.22	9.75
	Max	29.34	88.43	88.24	97.70	153.12	22.36	18.47
	Median	6.20	30.19	21.43	5.33	101.12	3.88	13.15
	Mean	10.20	31.78	38.97	27.05	98.32	6.57	13.34
	Std Dev	8.86	19.90	34.90	39.81	37.96	5.71	2.61
Zr	Min	212.84	252.70	259.23	243.08	242.43	281.02	230.86
	Max	289.58	306.30	305.31	294.44	277.31	307.10	236.64
	Median	266.64	274.61	268.99	272.53	253.41	303.90	232.45
	Mean	258.51	275.47	278.08	270.29	254.77	299.19	232.78
	Std Dev	27.31	10.08	19.65	13.48	8.88	9.11	1.95

Table 5. One-way ANOVA statistics for minor elements in all bead colors.

Element	Mean	F Ratio	DF	P
Fe	759.62	7.96	6	<0.001
Co	382.277	65.99	6	<0.001
Ni	73.75	2.00	6	0.07
Cu	2213.19	30.00	6	<0.001
Zn	1255.27	6.97	6	<0.001
As	524.19	18.80	6	<0.001
Pb	77.97	9.31	6	<0.001
Mn	513.01	78.99	6	<0.001
Ti	42.59	141.98	6	<0.001

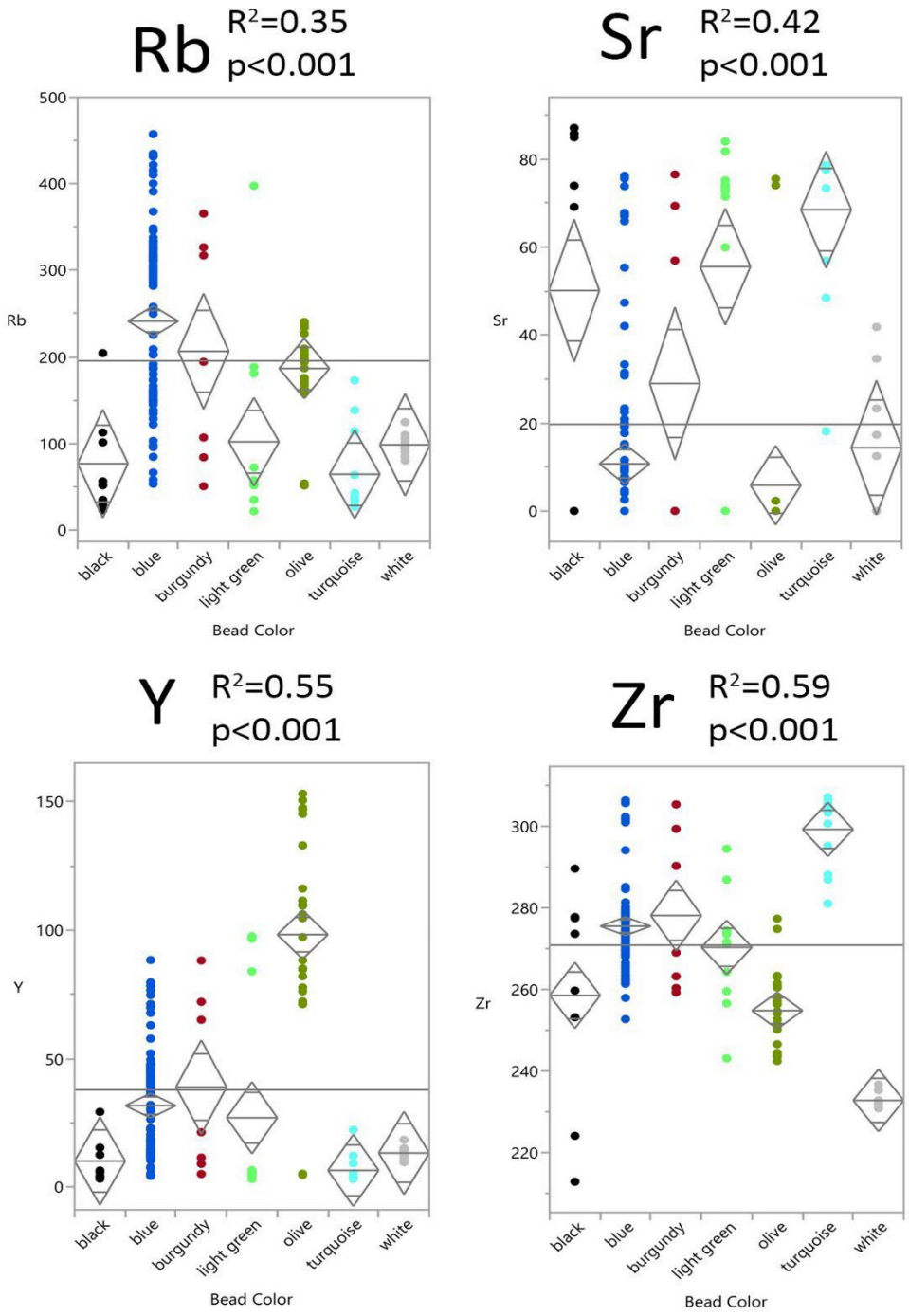

Figure 7. Box plot charts for trace elements Rb, Sr, Y, and Zr by bead color. Gray horizontal line is the mean for all beads. Each diamond shows the mean and standard deviations for each bead color.

green, olive, and turquoise all have content below the mean, and all the white beads are above the mean.

Trace elements associated with volcanic elements were also analyzed (Table 6). A visual representation of the results (Figure 7) shows higher concentrations of Rb in blue and burgundy beads. Concentrations of Sr are below the mean for blue, olive, and white beads. Only the olive beads have concentrations of Y above the mean and are widely distributed. Concentrations of Zr in all colors have wide distribution, with white beads all falling well below the mean.

Table 6. One-way ANOVA statistics for trace elements in all bead colors.

Element	Mean	F Ratio	DF	P
Rb	195.38	15.03	6	<0.001
Sr	19.71	20.17	6	<0.001
Y	37.92	34.19	6	<0.001
Zr	270.82	41.11	6	<0.001

In summary, XRF analysis indicates that Prosser bead colors have specific combinations of diagnostic major, minor, and trace elemental combinations that appear as either intentional additions to recipes or as natural geochemistry of the raw materials used. The absence of some elements in specific colors and presence in others indicate that that element was likely added deliberately to manipulate color. Grouped patterns of concentrations in basic elements indicate that distinctions can be made between manufacturing events that reflect either a difference in recipe, or a difference in raw material source. I explore these patterns in greater detail below.

Analysis

The purpose of this study is to determine whether an examination of elemental composition of Prosser beads can provide information on the geographical origins of the raw materials used to make the beads, thereby helping to identify the location and perhaps time of their manufacture. To this end, I will examine the elements in three different groups. First, I will analyze the elements in feldspar (Si, Al, Ca, and K) and quartz sand (Si), which are the major elements in the recipe for Prosser beads. Second, I will look at the presence of trace elements, particularly rubidium and strontium, which commonly replace K and Ca in feldspar. Finally, I will examine the elements commonly added to glass recipes as coloring agents. These three analyses will identify which elements have significant variation that can be interpreted as diagnostic of provenance.

Feldspar is an aluminosilicate mineral that consists of Al, Si, and a third alkali element, usually Ca, Na, or K. The ratios of So to Al vary from 1:1 to 3:1. The predictable chemistry of alkali feldspar provides a way to compare elemental contents of beads to suggest whether raw material sources for each bead are similar.

From the distribution chart showing each of the four elements in the collection (Figure 8), we can see that the ratio of Si to Al is roughly 7:1, indicating that all the beads were made with the addition of quartz sand to feldspar, as feldspar alone would not have more than 3:1 ratios of these elements, and kaolin clay ratios are generally 1:1 to 2:1 (Ross and Kerr 1931). Each of the four elements shows a wide distribution in beads with concentrations above the mean, with Si showing numerous high outliers. While it is

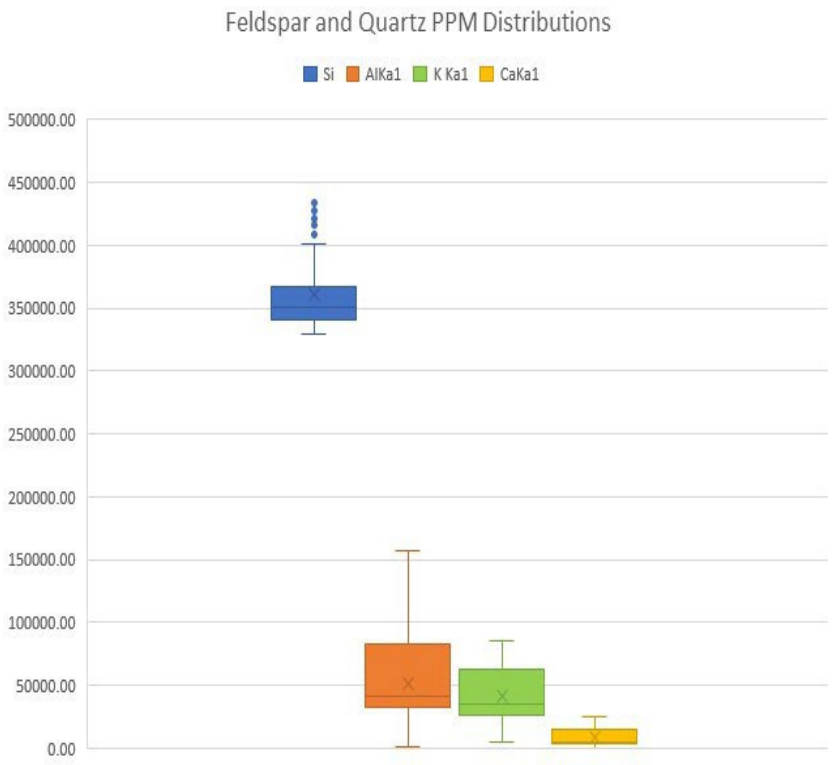

Figure 8. Comparison of quantified concentrations (ppm) of Si, Al, K, and Ca.

impossible to determine how much of the Si exists as the result of sand versus feldspar, the ratios indicate that the combination of the two minerals was the main part of the bead recipe as expected. Applying a smooth curve fit to the histograms reveals that each element has bimodal distribution (Figure 9), suggesting two potential provenances.

To evaluate each of the four elements in relation to each other, a scatterplot matrix was created (Figure 10). Each scatterplot shows distinct bead clusters, with a strong positive linear relationship between K and Al where the two clusters are clearly separated between low K (K<50,000 ppm) and high K (K>50,000 ppm). Selecting only

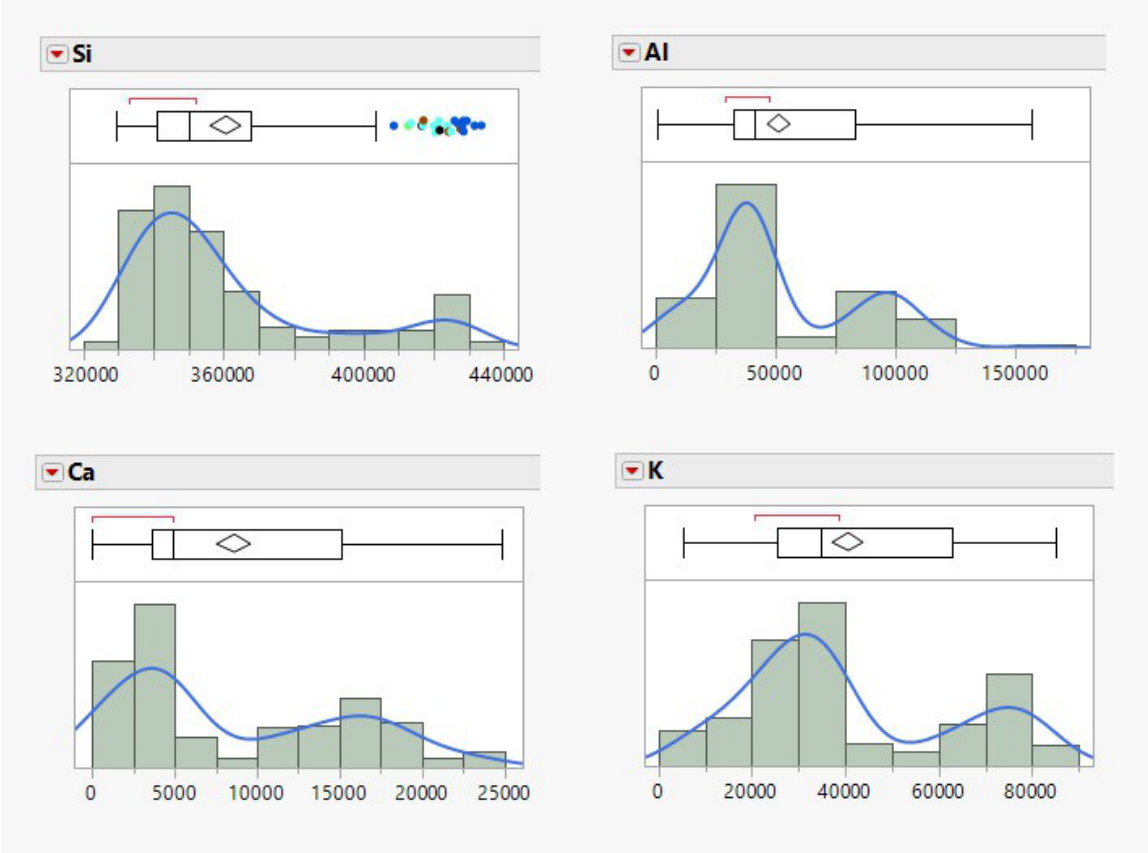

Figure 9. Histograms showing parts-per-million of Si, Al, Ca, and K. The graphs include a smooth curve fit line and horizontal box plot of distribution above each histogram.

the beads in the high K group demonstrates that these beads have distinct characteristics that are illustrated by their groupings in each of the other plots (Figure 11). The high K bead group consists of fifty blue beads, two burgundy beads, and one light green bead. In the following discussion, this distinct cluster of beads will be referred to as the "high K" beads and will be the same beads that are shown highlighted in subsequent figures.

Plotting K, Al, and Si in a ternary plot (Figure 12) shows a linear pattern with the high K beads showing decreased amounts of Si as K increases. Replacing Ca for Si on

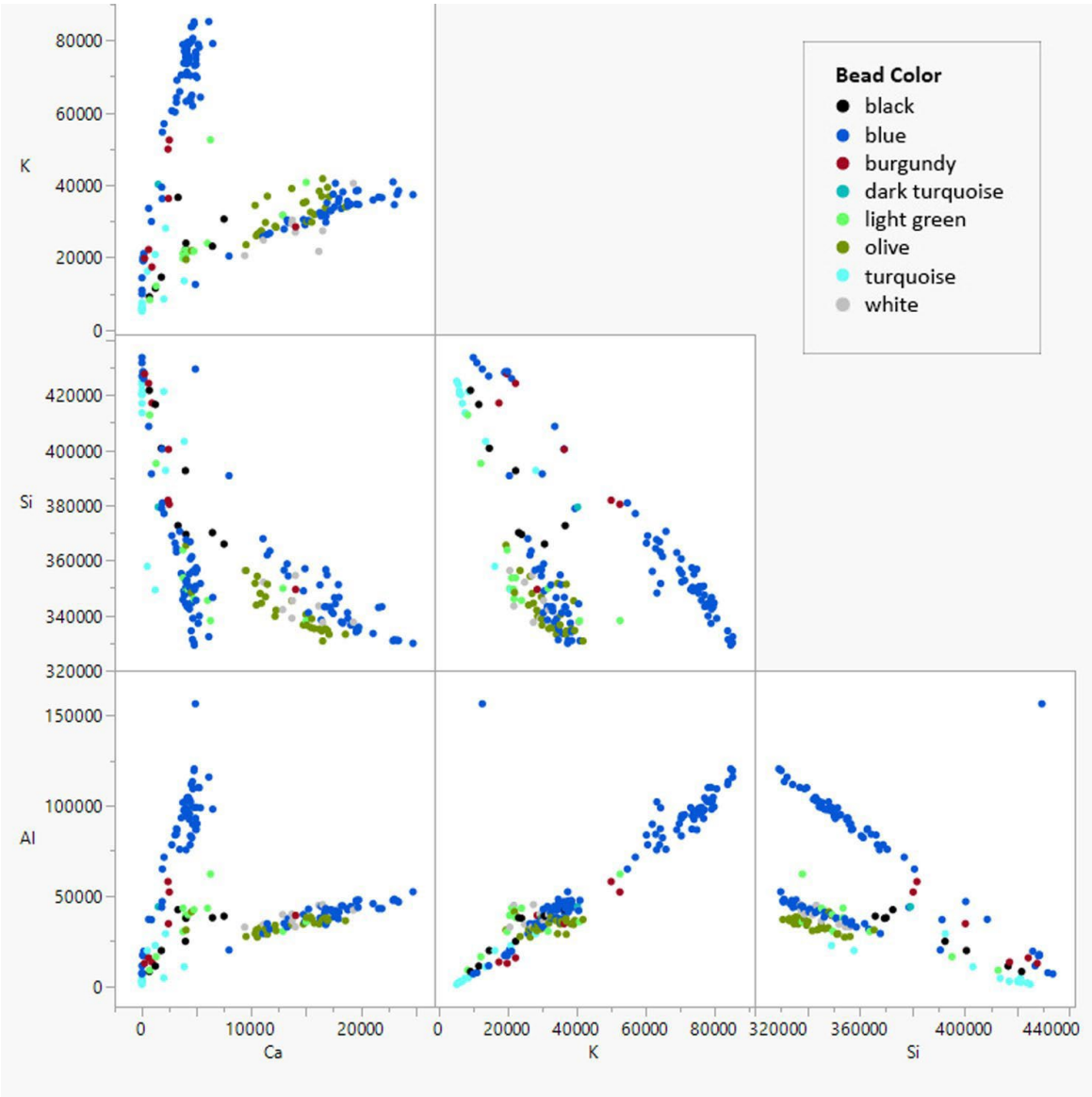

Figure 10. Scatterplot matrix showing relationships of Si, Al, Ca, and K. Dot colors represent bead colors as shown in legend.

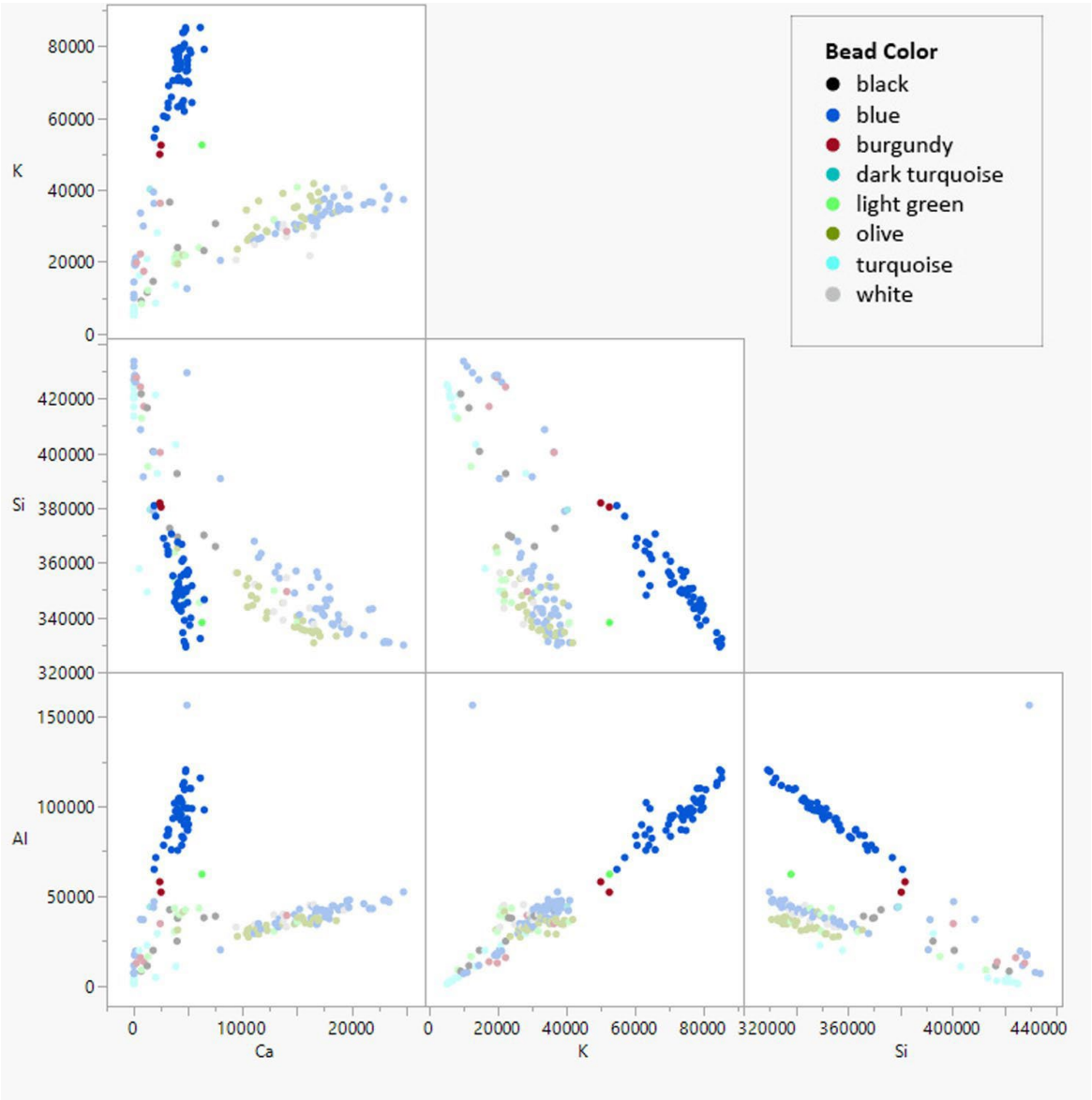

Figure 11. Scatterplot matrix showing relationships of Si, Al, Ca, and K. Highlighted dots represent high K beads (n=53) as determined by the bottom middle plot of Al and K. Dot colors represent bead colors as shown in legend.

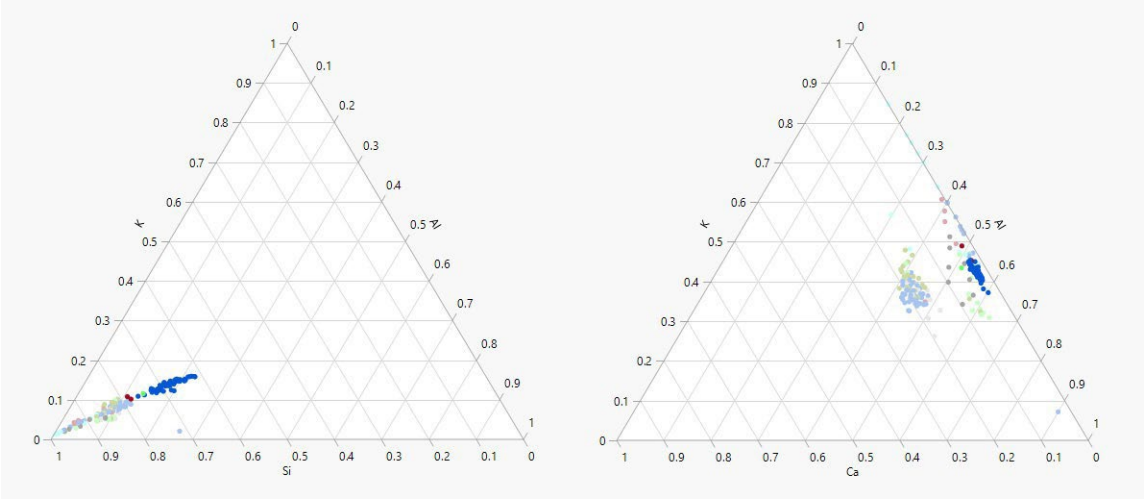

Figure 12. Ternary plot of K and Al over Si (left) showing linear relationships and ternary plot of K and Al over Ca (right) showing two distinct clusters of data. High K beads as defined previously are highlighted and dot colors represent bead colors as shown in legend.

the plot, however, shows distinct bead groupings, with the high K beads grouped in a lower Ca content cluster.

The grouping patterns in the statistical comparisons of beads in the context of Si, Al, Ca, and K strongly suggest variation in either basic recipes of the beads or distinct sources for feldspar as a raw material if the ratios of feldspar and quartz sand remain constant. In addition to Ca and K, alkali feldspars also may contain Na, and it is noted that the lack of data for this element is a weakness in this analysis. Nevertheless, the strong associations between Al and K indicate that some differentiation in manufacturing process (recipe or source) can be distinguished.

In alkali feldspar, other trace elements may occasionally replace the Ca/Na/K position in the chemical structure through various natural geologic processes (Ribbe 1975). Rubidium, for example, can replace K, or Sr can replace Ca, resulting in feldspar with distinct ratios of these two elements (Heier 1962). Four mid-Z elements (Rb, Sr, Zr,

and Y) typically associated with volcanic material are considered sensitive provenance indicators for obsidian (Glascock 2020). In the case of Prosser beads, they may appear in relation to the feldspar and in contrast to the alkali components analyzed above. The relationships between these four trace elements are first examined in a scatterplot matrix (Figure 13a). Strong clustering patterns can be seen in each comparison, suggesting that the relationships between the four elements are not random. Figure 13b is the same

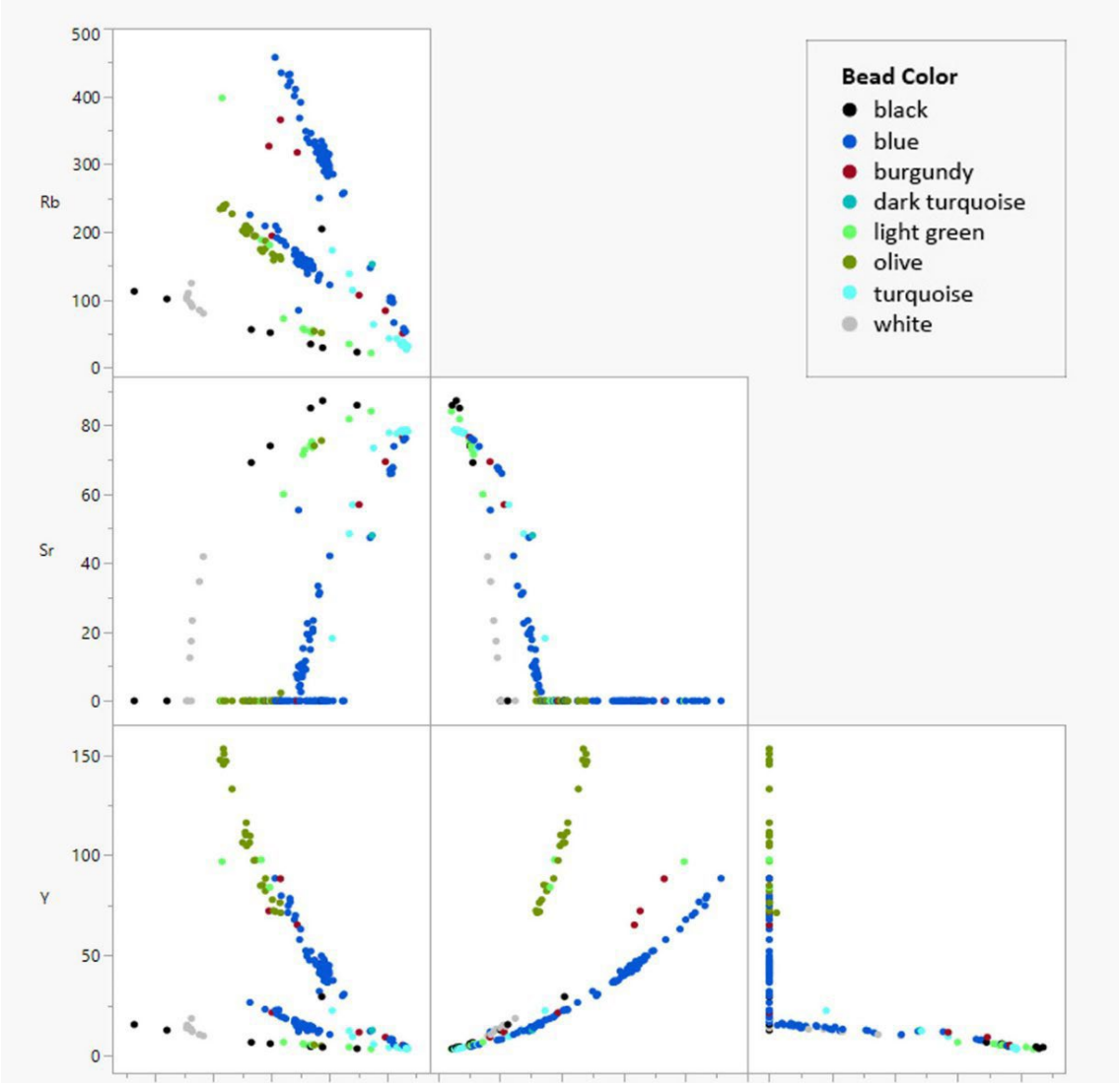

Figure 13a. Scatter plot matrix showing comparisons of trace elements Rb, Sr, Zr, and Y. Dot colors represent bead colors as shown in legend.

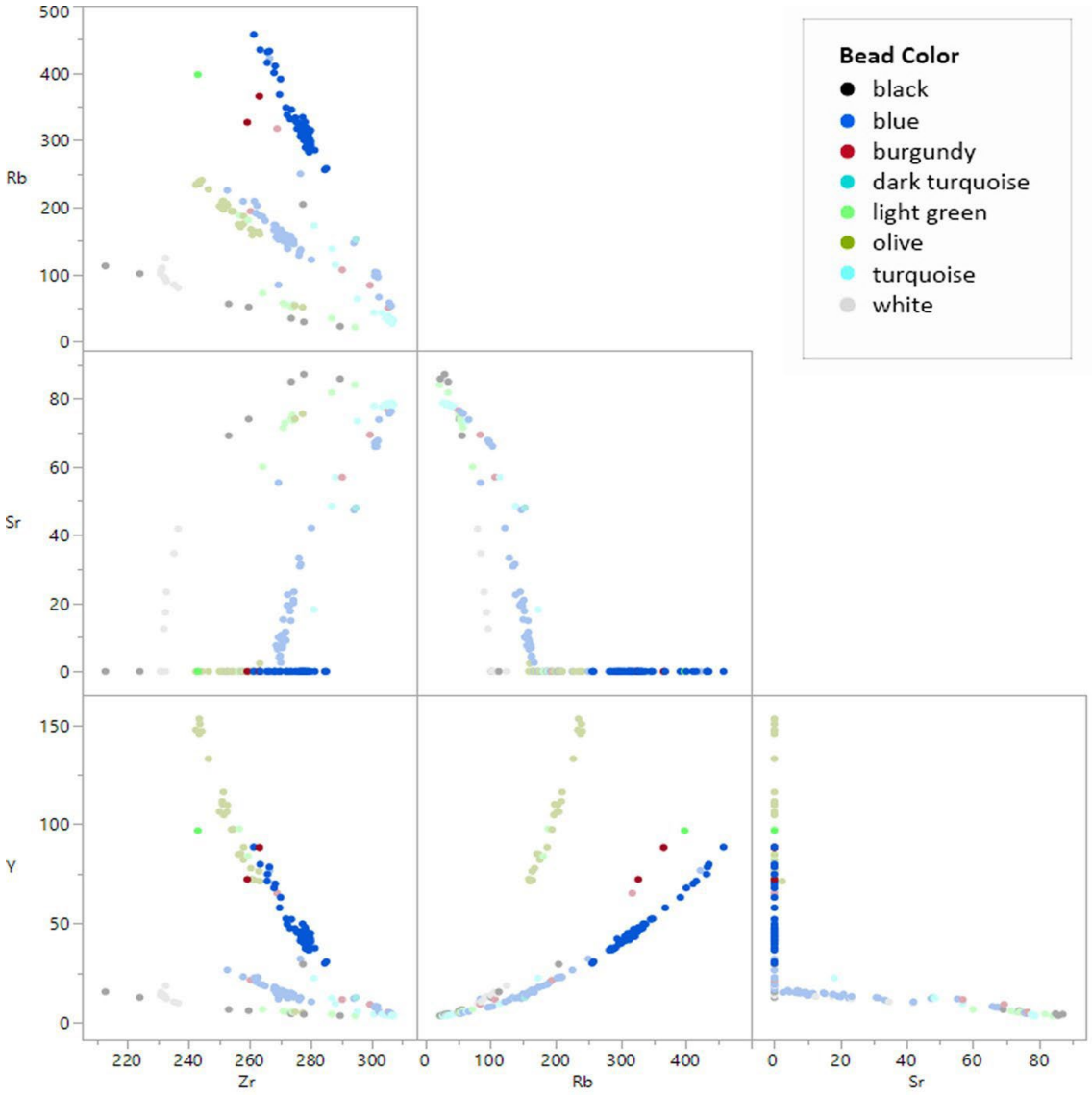

Figure 13b. Scatterplot matrix showing comparisons of trace elements Rb, Sr, Zr, and Y. High K beads as defined previously are highlighted and dot colors represent bead colors as shown in legend.

scatterplot matrix but the high K beads are highlighted. In each scatterplot, these beads maintain their clustered relationship, suggesting that their variation is correlated.

Principal component analysis (PCA) can be used to further understand the relationship between the mid-Z elements of Rb and Sr and the K and Ca they may

replace. These four elements are combined to create a visual representation of how their variability is correlated (Figure 14). Rubidium and potassium have vectors that are very

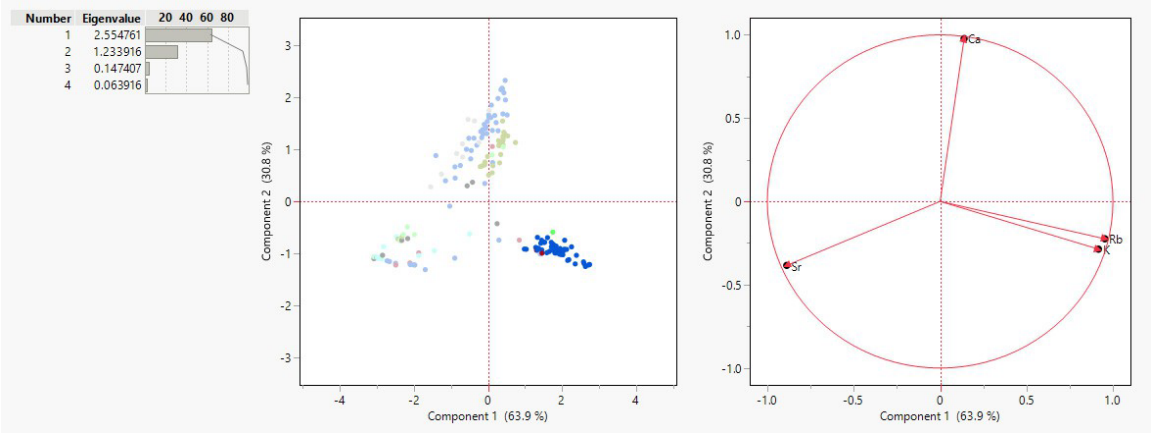

Figure 14. Principal component analysis of Rb, K, Sr, and Ca. Strong correlation is shown between Rb and K, while Sr and Ca, with vectors at approximately right angles are not correlated. Highlighted beads on the scatterplot are the same high K as previously noted and dot colors represent bead colors as shown in legend.

closely aligned, indicating that they are strongly correlated. Strontium and potassium, however, are vectors that appear at approximately right angles to Rb and Sr as well as to each other, indicating they are not correlated. The accompanying PCA scatterplot shows that the high K beads previously identified are grouped in the lower right quadrant. Two other clusters are shown, which suggests the presence of at least three groups that co-vary.

Major elements and trace elements appear because of natural occurrences in the raw materials, but coloring agents occur as the result of deliberate decision-making of the manufacturer. Beads of the same color made in the same place with the same raw materials and recipe should have consistent amounts of coloring agents for each color. Otherwise, variation of these elements suggests some intentional difference at the

manufacturing level. Color variations in glass are obtained using various elements. Cobalt and copper are most used for blue and green, and combinations of the two elements can produce a variety of shades. Zinc and titanium may be used to produce white, and iron can produce red colors. Beads of the same color are expected to contain similar amounts of coloring agents to obtain similar colors.

In a scatterplot matrix of these elements (Figure 15), we would expect that beads of the same color fall into groups reflecting the intentional coloring of the material.

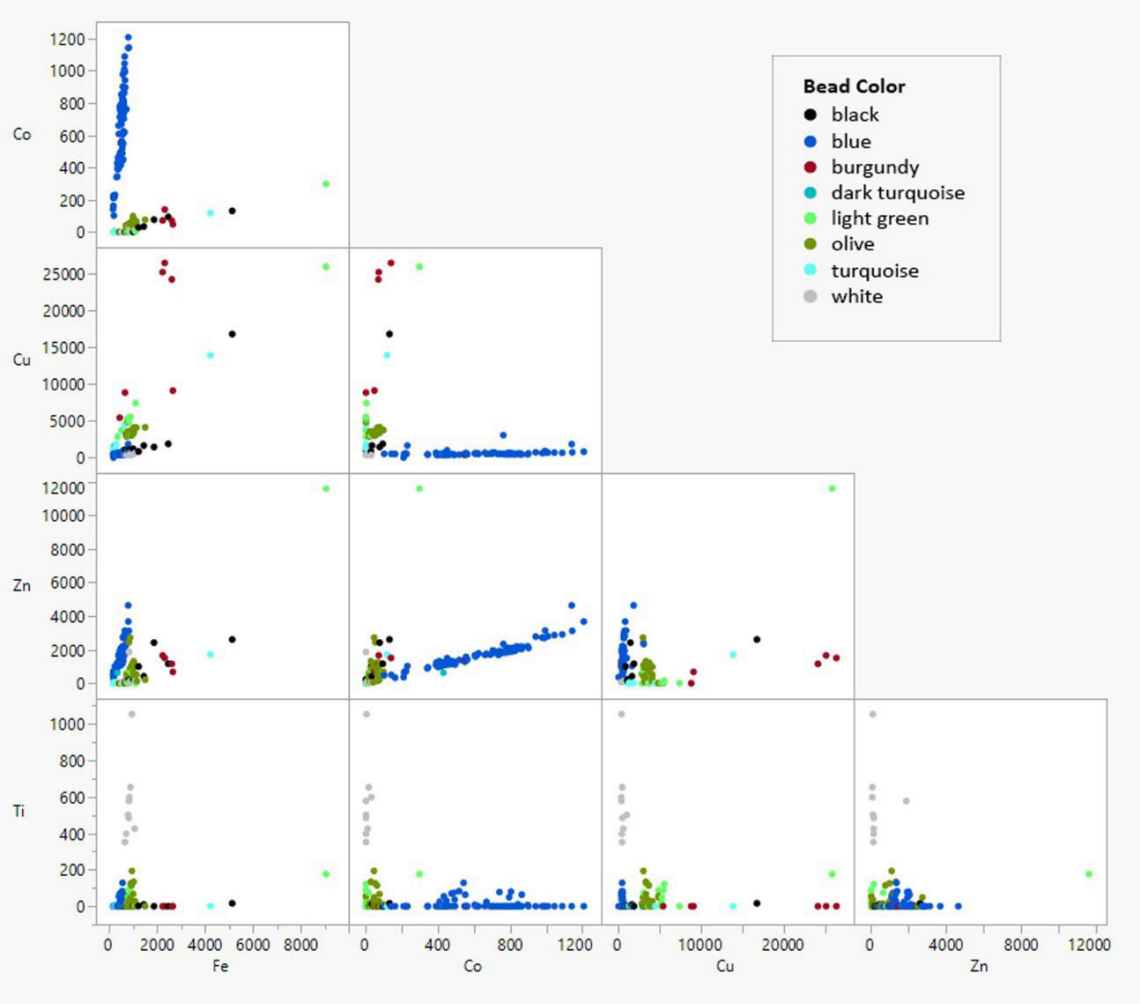

Figure 15. Scatterplot matrix of coloring elements Co, Cu, Zn, Ti, and Fe. Colors of beads are tightly grouped except for blue beads, which have high variation of cobalt. Dot colors represent bead colors as shown in legend.

While the olive-green beads indeed seem to group together, blue and white beads show wide variation in Co and Ti respectively, and burgundy beads show wide variation in Cu content. Since the coloring elements are intentionally added to the bead mixtures, significant variation must also reflect intentional differences. The blue beads have been shown to appear in at least two clusters in the previous elemental analyses (see Figures 10, 11, 12, 13 and 14). This distinction is shown clearly in a bivariate plot of Co against K, a major element which has been shown above to be a diagnostic element in the analysis that impacts variation (Figure 16).

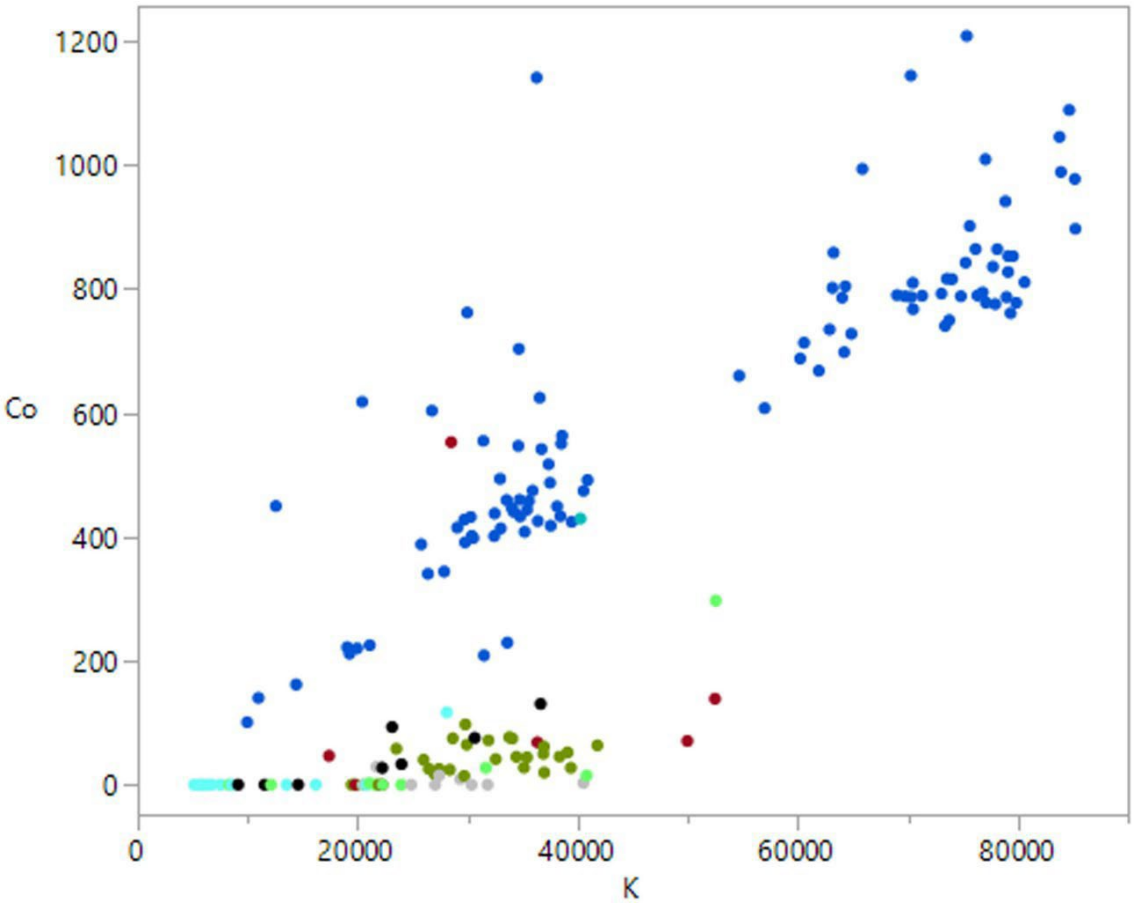

Figure 16. Bivariate plot of Co and K. The dot color corresponds to bead color. Two distinct groups of blue beads are evident, one with higher and one with lower K content.

Since coloring agents are added with intention rather than occurring naturally, the color of the beads can be used as a control variable in the analysis of other elements. Returning to the ternary plot of the major elements Al, Ca, and K, the blue beads are seen to divide into two distinct groups (Figure 17). Each group of blue beads has different amounts of Co, which does not influence the color visually. Nevertheless, the beads with lower K also have lower Co content, and the high K beads have higher Co, as shown in Figure 17 by the histograms for each, indicating co-variance.

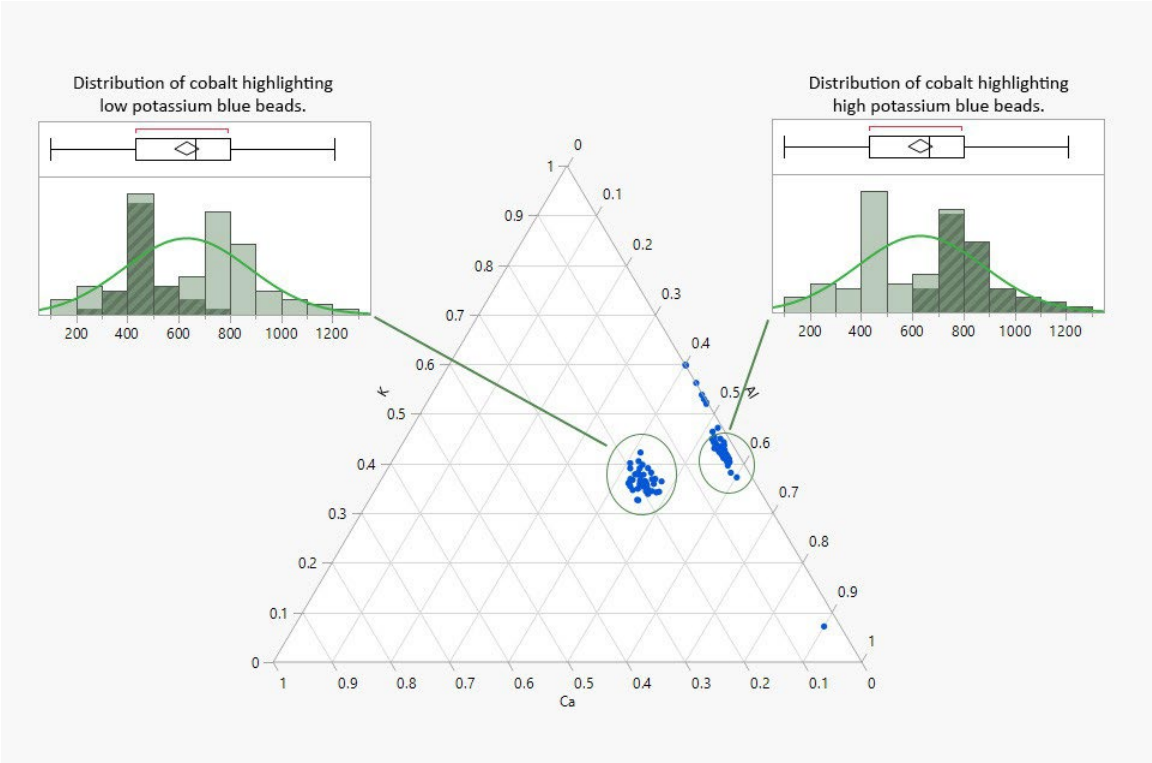

Figure 17. Ternary plot of K and Al over Ca showing variance of blue beads only with cobalt distribution. The histograms show sub-distribution (hatch-marked) of cobalt for the respective cluster of beads as indicated.

Discussion

The above analysis demonstrates that at least two and probably three chemically distinct groupings exist in the analyzed bead sample. Several possibilities can be considered to explain why these distinctions exist. Variation in raw materials occur naturally which might reflect different raw material sources. For example, after World War II, the Bapterosses factory sold the Norwegian feldspar mine and turned to more local sources (Nourisson 2001). Additionally, deliberate addition of elements to satisfy color recipes could indicate distinct manufacturing practices of different factories and may correspond to various raw material sources. Recipes would likely vary from one company to another but may also vary within one company. Internal adjustments could occur over time as recipes were refined, as access to resources changed, or even as workers were more or less consistent in their practice.

Naturally occurring elements in feldspar exist because of variation in geological formations and are expected to represent various raw material sources as opposed to intentional variation resulting from different recipes. Ratios of various major, minor, and trace elements should be consistent in beads from the same factory using the same raw material source and recipe. The Bapterosses factory in Briare owned a Feldspar mine and imposed strict quality controls on bead production (Nourisson 2001). The Redlhammer factory in Gablonz made multiple changes to factory operations (Neuwirth 2011), suggesting that quality control and raw material sourcing was less important to the final

product. As a result, beads from Briare might be expected to show element relationships that are more tightly grouped, and beads from Gablonz may have more variation in the same relationships. Without examples from each of the two factories it is not possible to verify that patterns are associated with one location or another. Nevertheless, distinct groupings of elements that persist in individual beads across elemental comparisons indicate that distinction can be made.

The grouping of the same beads in different analyses reflects concordant variation that indicates these beads are chemically distinguishable. In each of three analyses, bivariate comparisons revealed elements that either had strong linear relationships, or that varied in opposition. Potassium and aluminum were found to have a strong positive linear relationship, suggesting that their variation was linked chemically. Strontium had an opposite relationship to other trace elements analyzed. Rubidium strongly corresponded to the variation in K, while Sr and Ca were not correlated in the PCA. Blue beads colored with a wide variation of Co served to demonstrate that the variations existed independent of recipes for color.

Conclusion

Detailed quantitative analysis shows patterns of concordant variation in elemental composition among the 211 beads evaluated. While more than two groups seem to exist, a distinct group of 53 beads show concordant variation across multiple chemical

configurations. These 53 beads retain their elemental relationships in a consistent cluster across multiple statistical analyses.

This group of distinct beads, and other potential clusters shown in the graphs, are the result of either different raw material sources, or different manufacturing practices. Further study of Prosser beads using XRF with a helium flush to include detection of sodium will provide additional insight into these analyses. Additionally, beads with known provenance can be assessed to determine if variations exist at the inter-factory level, or if they are specific to each manufacturing location.

Given these results, it is a reasonable conclusion that with further study and development, elemental models may be created that will provide researchers with a way to establish provenance of Prosser beads using XRF technology in the field. Pre- and post-WWII time periods may also be distinguished. Such models will provide valuable insight into manufacturing, material procurement, and international distribution and sales practices in the 19th and 20th centuries across three continents.

References Cited

Adlington, Laura W.

2017 The Corning Archaeological Reference Glasses: New Values for "Old" Compositions. Papers from the Institute of Archaeology, 27:1-8.

Adlington, Laura W., I. C. Freestone, J. J. Kunicki-Goldfinger, T. Ayers, H Gilderdale Scott, and A. Eavis

2019 Regional Patterns in Medieval European Glass Composition as a Provenancing Tool. *Journal of Archaeological Science*, 110:104991.

Andrén, Anders

1998 *Between Artifacts and Texts: Historical Archaeology in Global Perspective*. Plenum Press, New York.

Beck, Horace C.

1928 Classification and Nomenclature of Beads and Pendants. *Archaeologia*, 77:1-76.

Blair, Elliot H.

2017 An XRF Compositional Analysis of Opaque White Glass Beads from 17th-Century Mission Santa Cataline de Guale, Georgia. *BEADS: Journal of the Society of Bead Researchers*, 29:31-48.

2022 pXRF Analysis of Heritage Glass. In *Advances in Portable X-Ray Fluorescence Spectrometry: Instrumentation, Application and Interpretation,* edited by Lee B. Drake and Brandi L. MacDonald, pp. 400-423. Royal Society of Chemistry, London.

Brill, Robert H.

1999 *Chemical Analyses of Early Glasses*. Corning Museum of Glass, Corning, NY.

Dadiego, Danielle L., Alyssa Gelinas and Tsim D. Schneider

2021 Unpacking the Bead: Exploring a Glass Bead Assemblage from Mission Santa Cruz, California, Using LA-ICP-MS. *American Antiquity*, 86(2):413-424.

Drake, B. Lee, and Brandi L. MacDonald

2022 *Advances in Portable X-Ray Fluorescence Spectrometry: Instrumentation, Application and Interpretation*. Royal Society of Chemistry, London.

Dussubieux, Laure and Heather Walder

2022 *The Elemental Analysis of Glass Beads: Technology, Chronology and Exchange*. Leuven University Press, Leuven, Belgium.

Glascock, Michael D.

2011 Comparison and Contrast Between XRF and NAA: Used for Characterization of Obsidian Sources in Central Mexico. In *X-Ray Fluorescence Spectrometry (XRF) in Geoarchaeology*, edited by M. Steven Shackley, pp. 161-192. Springer, New York.

2020 A Systematic Approach to Geochemical Sourcing of Obsidian Artifacts. *Scientific Culture*, 6(2):35-47.

Hancock, Ronald G. V., A. Chafe, and Ian Kenyon

1994 Neutron Activation Analysis of Sixteenth-and Seventeenth-Century European Blue Glass Trade Beads from the Eastern Great Lakes Region of North America. *Archaeometry*, 36 (2):253-266.

Hancock, Ronald G. V., Susanne Aufreiter, and Ian Kenyon.

1997 European White Glass Trade Beads as Chronological and Trade Markers. MRS Proceedings, 462:181-191.

Hancock, Ronald G. V., J. McKechnie, Susanne Aufreiter, Karlis Karklins, M. Kapaches, M. Sempowski, Jean-Francois Moreau, and I. Kenyon

2000 Non-Destructive Analysis of European Cobalt Blue Glass Trade Beads. *Journal of Radioanalytical and Nuclear Chemistry*, 244:567-573.

Hancock, Ronald G. V.

2005 Elemental Analyses of North American Glass Trade Beads. *BEADS: Journal of the Society of Bead Researchers,* 17:52-57.

Heier, Knut S.

1962 Trace Elements in Feldspars – A Review. *Norsk Geologisk Tidsskr* 42:415-454.

Johnson, Lucas R. Martindale, Jeffrey R. Ferguson, Kyle P. Freund, Lee Drake, and Daron Duke

2021 Evaluating Obsidian Calibration Sets with Portable X-Ray Fluorescence (ED-XRF) Instruments. *Journal of Archaeological Science: Reports*, 39:103126.

Kaspers, Floor

2011 *Beads from Briare*. Marblings Publishing, Amsterdam.

2014 *Beads from Jablonec*. Marblings Publishing, Amsterdam.

Karklins, Karlis

1992 Identifying Beads Used in the 19th-Century Central East Africa Trade. *BEADS: Journal of the Society of Bead Researchers,* 4:49-59.

2012 Guide to the Description and Classification of Glass Beads Found in the Americas. *BEADS: Journal of the Society of Bead Researchers* 24:62-90.

Kenyon, Ian T., Ronald G. V. Hancock, and S. Aufreiter

1995 Neutron Activation Analysis of A.D. 1600-1930 European Copper-Coloured Blue Glass Trade Beads from Ontario, Canada. *Archaeometry*, 37(2):323-337.

Kirkish, Alex N.
2014 Prosser Beads from the Mission San Gabriel Arcángel (Ca-Lan-184h). *Proceedings of the Society for California Archaeology* 28:311-317.

Kidd, Kenneth E., and Martha Ann Kidd
1970 A Classification System for Glass Beads for the Use of Field Archaeologists. *Canadian Historic Sites: Occasional Papers in Archaeology and History*, 1:45-89.

Michelaki, K., and R. G. V. Hancock
2011 Chemistry Versus Data Dispersion: Is There a Better Way to Assess and Interpret Archaeometric Data? *Archaeometry*, 53(6):1259-1279.

Neuwirth, Waltraud
2011 Beads from Gablonz. *BEADS: Journal of the Society of Bead Researchers*, 23:3-111.

Nourisson, Pascale
2001 *Une Aventure Industrielle: La Manufacture de Briare (1837-1962)*. Éditions Alan Sutton, Saint-Avertin, France.

Opper, Marie-José and Howard Opper
1991 French Beadmaking: An Historic Perspective Emphasizing the 19th and 20th Centuries. *BEADS: Journal of the Society of Bead Researchers*, 3:47-59.

1993 Powdered-Glass Beads and Bead Trade in Mauritania. *BEADS: Journal of the Society of Bead Researchers*, 5:37-44.

Orchard, William C.

1975 *Beads and Beadwork of the American Indians.* Museum of the American Indian & Heye Foundation.

Panich, Lee M.

2014 Native American Consumption of Shell and Glass Beads at Mission Santa Clara De Asís. *American Antiquity* 79(4):730-748.

Ribbe, Paul H. (editor)

1975 *Feldspar Mineralogy*. Mineralogical Society of America, Chelsea, Michigan.

Ross, C.S. and P. F. Kerr

1931 The Kaolin Minerals, Professional Paper 165-E. *Shorter Contributions to General Geology*, U.S. Geological Survey Publications.

Ross, Lester A.

1990 Trade Beads from Hudson's Bay Company Fort Vancouver (1829-1860), Vancouver, Washington. *BEADS: Journal of the Society of Bead Researchers*, 2:29-67.

Sempowski, Martha L., A. W. Nohe, J.-F. Moreau, I. Kenyon, Karlis Karklins, and Ron G. V. Hancock

2000 On the Transition from Tin-Rich to Antimony-Rich European White Soda-Glass Trade Beads for the Senecas of Northeastern North America. *Journal of Radioanalytical and Nuclear Chemistry* 244:559–566.

Shackley, Steven

2011 *X-Ray Fluorescence Spectrometry (XRF) in Geoarchaeology*. Springer, New York.

Shugar, Aaron and Ariel O'Connor

2008 The Analysis of 18th Century Glass Trade Beads from Fort Niagra: Insight Into Compositional Variation and Manufacturing Techniques. *Northeast Historical Archaeology*, 37(1):58-68.

Sprague, Roderick

1983 Tile Bead Manufacturing. In *Proceedings of the 1982 Glass Trade Bead Conference*, edited by Charles F. Hayes III, pp. 167-172. Rochester Museum and Science Center, Rochester.

2002 China or Prosser Button Identification and Dating. *Historical Archaeology*, 36(2):111-127.

Thiry, Médard and Benoît Maréchal

2001 Development of Tightly Cemented Sandstone Lenses in Uncemented Sand: Example of the Fontainbleau Sand (Oligocene) in the Paris Basin. *Journal of Sedimentary Research*, 71(3):473-483.

Vicenzi, Edward P., Stephen Eggins, Amelia Logan, and Richard Wysoczanski

2002 Microbeam Characterization of Corning Archaeological Reference Glasses: New Additions to the Smithsonian Microbeam Standard Collection. *Journal of Research of the National Institute of Standards and Technology*, 107(6):719-727.

Walder, Heather

2018 Small Beads, Big Picture: Assessing Chronology, Exchange, and Population Movement through Compositional Analyses of Blue Glass Beads from the Upper Great Lakes. *Historical Archaeology*, 52:3301-331.

Walder, Heather, Joseph A. Petrus, Laure Dussubieux, Ronald G. V. Hancock, and Alicia L. Hawkins

2021 Comparing Chemistries: Inter-Laboratory Evaluation of Glass Bead Compositional Research in the Great Lakes Region. *Archaeometry*, 63(6):1236-1254.

Yatsuk, Oleh, Marco Ferretti, Astrik Gorghinian, Giacomo Fiocco, Marco Malagodi, Angelo Agostina, and Monica Gulmini

2022 Data from Multiple Portable XRF Units and Their Significance for Ancient Glass Studies. *Molecules*, 27(18):6068.